Performance of Transportation Infrastructure During Kumamoto Earthquakes of April 14 and 16, 2016—A Reconnaissance Report

PUBLICATION NO. FHWA-HRT-22-110

MARCH 2023

U.S. Department of Transportation
Federal Highway Administration

Research, Development, and Technology
Turner-Fairbank Highway Research Center
6300 Georgetown Pike
McLean, VA 22101-2296

FOREWORD

Determining the engineering performance of the highway infrastructure, especially following extreme events, is key to improving design and construction practices, thereby providing improved safety to the traveling public. On April 14 and 16, 2016, the Kumamoto Prefecture on the Japanese island of Kyushu experienced two very large earthquakes, a magnitude 6.5 followed 28 h later by a magnitude 7.3. These earthquakes caused extensive damage to the built infrastructure, including the transportation infrastructure. At the request of Japan, the Federal Highway Administration organized a Transportation Infrastructure Reconnaissance Team to assess damage to bridges and other highway structures. This report presents the findings of the team during the reconnaissance. It describes the performance of new bridges that had been recently designed and older bridges that had been retrofitted for earthquakes.

This report will be useful to bridge owners, practicing engineers, and researchers. Lessons learned will be useful for improving the resilience of bridges so that lives may be saved in future extreme events.

Cheryl Allen Richter, P.E., Ph.D.
Director, Office of Infrastructure Research and Development

.

TECHNICAL REPORT DOCUMENTATION PAGE

1. Report No. FHWA-HRT-22-110	2. Government Accession No.	3. Recipient's Catalog No.
4. Title and Subtitle Performance of Transportation Infrastructure During Kumamoto Earthquakes of April 14 and 16, 2016—A Reconnaissance Report		5. Report Date March 2023 6. Performing Organization Code:
7. Author(s) Ron Bromenschenkel, Ian G. Buckle, Jim Cuthbertson, Sheila Rimal Duwadi, Denis Istrati, and David H. Sanders		8. Performing Organization Report No.
9. Performing Organization Name and Address Turner-Fairbank Highway Research Center Federal Highway Administration 6300 Georgetown Pike, McLean, VA 22101 Department of Civil and Environmental Engineering University of Nevada Reno 1664 N. Virginia Street Reno, NV 89557 Geotechnical Office Washington State Department of Transportation 310 Maple Park Avenue SE P.O. Box 47300 Olympia, WA 98504 Office of Earthquake Engineering California Department of Transportation P.O. Box 942873 Sacramento, CA 95816		10. Work Unit No. 11. Contract or Grant No. DTFH61-07-00031
12. Sponsoring Agency Name and Address Office of Infrastructure Research and Development Federal Highway Administration 6300 Georgetown Pike, McLean, VA 22101-2296		13. Type of Report and Period Covered Final Report; July 2016 14. Sponsoring Agency Code HRDI-30
15. Supplementary Notes The Contracting Officer's Representative was Jamie Harris (HRDI-30).		
16. Abstract This report described a reconnaissance effort to document bridge performance during the Kumamoto earthquakes in Japan in April 2016. More than 180 bridges were damaged by these earthquakes. Of particular interest is the performance of bridges that were relatively new (15–20 yr old) or recently retrofitted. Damage sustained was significant and included bearing and shear key failures, distortion and local buckling of the steel superstructures, and foundation movement. Most of the damage could be attributed to extensive slope failures and intense shaking close to the causative fault. Recommendations for improving bridge performance in future earthquakes are given.		
17. Key Words Seismic performance, new bridges, retrofitted bridges, ground motion, ground failures, reconnaissance	18. Distribution Statement: No restrictions. This document is available through the National Technical Information Service, Springfield, VA 22161. http://www.ntis.gov	
19. Security Classif. (of this report) Unclassified	20. Security Classif. (of this page) Unclassified	21. No. of Pages 131 22. Price N/A

Form DOT F 1700.7 (8-72) Reproduction of completed page authorized.

SI* (MODERN METRIC) CONVERSION FACTORS

APPROXIMATE CONVERSIONS TO SI UNITS

Symbol	When You Know	Multiply By	To Find	Symbol
		LENGTH		
in	inches	25.4	millimeters	mm
ft	feet	0.305	meters	m
yd	yards	0.914	meters	m
mi	miles	1.61	kilometers	km
		AREA		
in^2	square inches	645.2	square millimeters	mm^2
ft^2	square feet	0.093	square meters	m^2
yd^2	square yard	0.836	square meters	m^2
ac	acres	0.405	hectares	ha
mi^2	square miles	2.59	square kilometers	km^2
		VOLUME		
fl oz	fluid ounces	29.57	milliliters	mL
gal	gallons	3.785	liters	L
ft^3	cubic feet	0.028	cubic meters	m^3
yd^3	cubic yards	0.765	cubic meters	m^3
	NOTE: volumes greater than 1,000 L shall be shown in m^3			
		MASS		
oz	ounces	28.35	grams	g
lb	pounds	0.454	kilograms	kg
T	short tons (2,000 lb)	0.907	megagrams (or "metric ton")	Mg (or "t")
		TEMPERATURE (exact degrees)		
°F	Fahrenheit	5 (F-32)/9 or (F-32)/1.8	Celsius	°C
		ILLUMINATION		
fc	foot-candles	10.76	lux	lx
fl	foot-Lamberts	3.426	$candela/m^2$	cd/m^2
		FORCE and PRESSURE or STRESS		
lbf	poundforce	4.45	newtons	N
lbf/in^2	poundforce per square inch	6.89	kilopascals	kPa

APPROXIMATE CONVERSIONS FROM SI UNITS

Symbol	When You Know	Multiply By	To Find	Symbol
		LENGTH		
mm	millimeters	0.039	inches	in
m	meters	3.28	feet	ft
m	meters	1.09	yards	yd
km	kilometers	0.621	miles	mi
		AREA		
mm^2	square millimeters	0.0016	square inches	in^2
m^2	square meters	10.764	square feet	ft^2
m^2	square meters	1.195	square yards	yd^2
ha	hectares	2.47	acres	ac
km^2	square kilometers	0.386	square miles	mi^2
		VOLUME		
mL	milliliters	0.034	fluid ounces	fl oz
L	liters	0.264	gallons	gal
m^3	cubic meters	35.314	cubic feet	ft^3
m^3	cubic meters	1.307	cubic yards	yd^3
		MASS		
g	grams	0.035	ounces	oz
kg	kilograms	2.202	pounds	lb
Mg (or "t")	megagrams (or "metric ton")	1.103	short tons (2,000 lb)	T
		TEMPERATURE (exact degrees)		
°C	Celsius	1.8C+32	Fahrenheit	°F
		ILLUMINATION		
lx	lux	0.0929	foot-candles	fc
cd/m^2	candela/m2	0.2919	foot-Lamberts	fl
		FORCE and PRESSURE or STRESS		
N	newtons	2.225	poundforce	lbf
kPa	kilopascals	0.145	poundforce per square inch	lbf/in^2

*SI is the symbol for International System of Units. Appropriate rounding should be made to comply with Section 4 of ASTM E380. (Revised March 2003)

TABLE OF CONTENTS

LIST OF FIGURES

LIST OF TABLES

LIST OF ABBREVIATIONS

EW	east-west
FHWA	Federal Highway Administration
JMA	Japan Meteorological Agency
JRA	Japan Road Association
JST	Japan Standard Time
KiK-net	Kiban Kyoshin
K-NET	Kyoshin
M	magnitude
MLIT	Ministry of Land, Infrastructure and Transport, and Tourism
Mw	moment magnitude
NE	northeast
NIED	National Research Institute for Earth Science and Disaster Resilience
NILIM	National Institute for Land and Infrastructure Management
NS	north-south
NW	northwest
PSP	Philippine Sea
PWRI	Public Works Research Institute
SE	southeast
SPL	seismic performance levels
SW	southwest
USGS	U.S. Geological Survey
UTC	Coordinated Universal Time
yBP	years before present

CHAPTER 1. INTRODUCTION

BACKGROUND

Japan is situated near the intersection of the Eurasia, Philippine Sea (PSP), Pacific, and North American Plates (figure 1). Japan is, therefore, susceptible to earthquakes. On April 14 and 16, 2016, the Kumamoto Prefecture on the island of Kyushu experienced two very large earthquakes, a magnitude (M) of 6.5 followed 28 h later by a M7.3. These earthquakes occurred several hundred kilometers northwest (NW) of the Ryukyu Trench, where the PSP begins its northwestward subduction beneath Japan and the Eurasia Plate (figure 2 and figure 3). Movement occurred on two mapped fault zones, Futagawa and Hinagu, as discussed in detail in chapter 2. The faults in the region generally trend east-west (EW) or northeast (NE)-southwest (SW). The strongest shaking was reported in the EW direction for the two earthquakes, with significant vertical, in addition to horizontal, acceleration. Peak motions exceeded design acceleration response spectra over a certain range of the natural period. The result was permanent horizontal and vertical ground displacement of 1–2 yd (1–2 m).

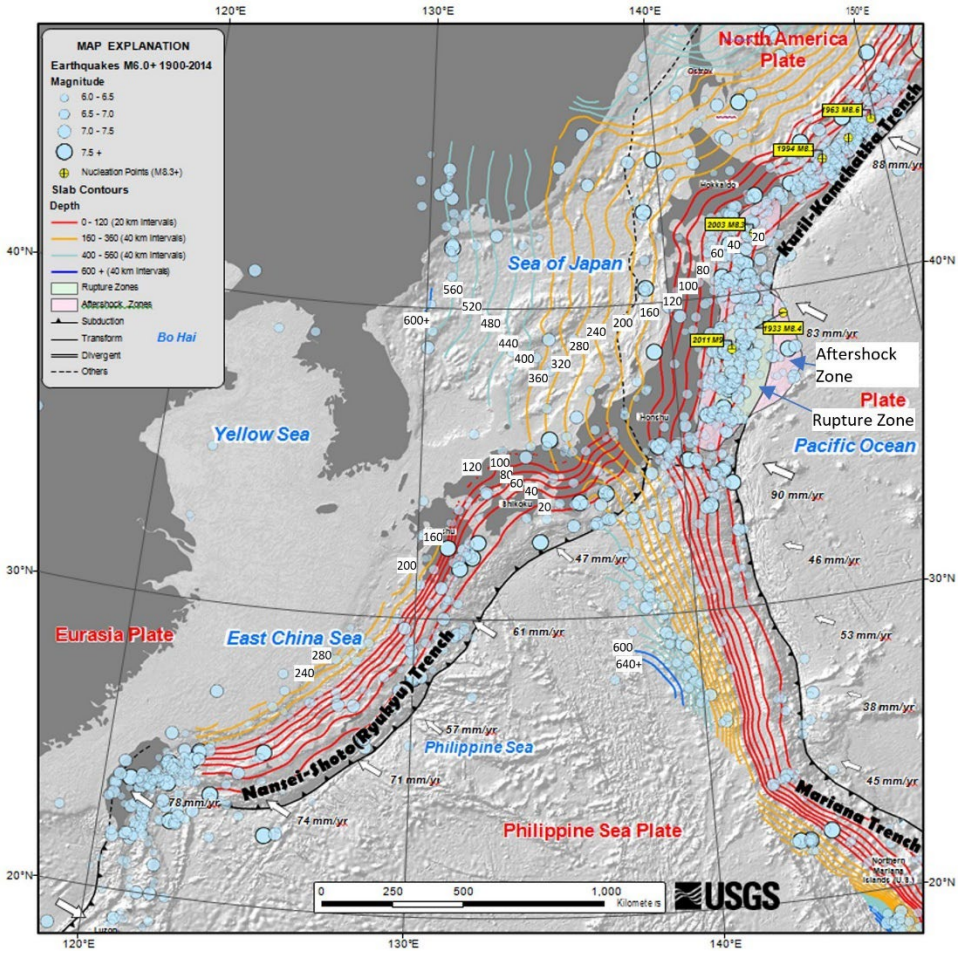

Source: U.S. Geological Survey (USGS).

Figure 1. Map. Tectonic map of Japan.

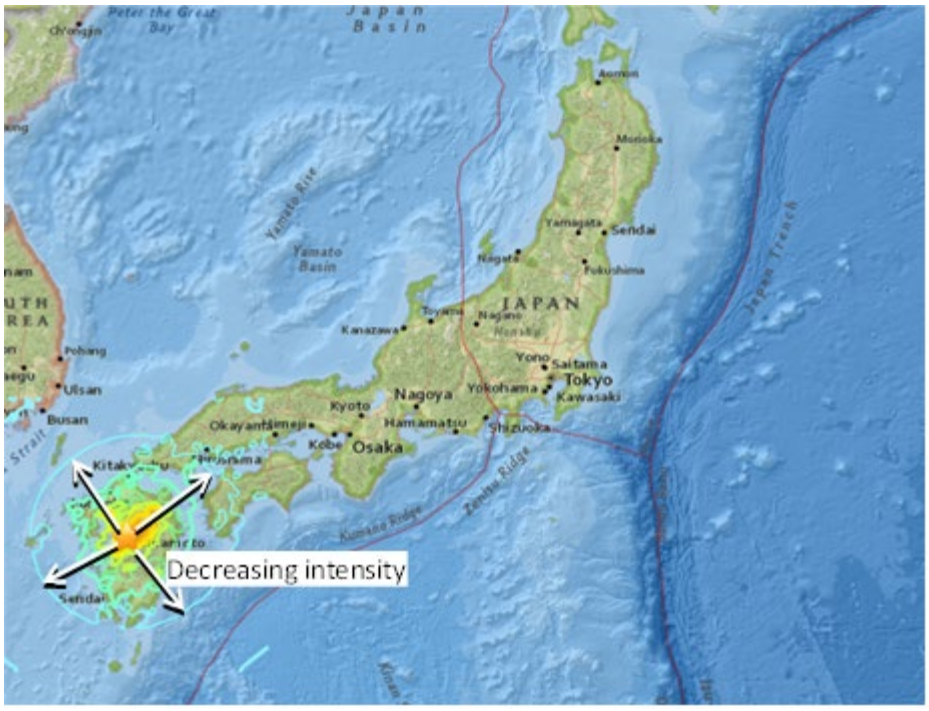

Source: USGS.

Figure 2. Map. Epicentral region of Kumamoto earthquakes, Japan.

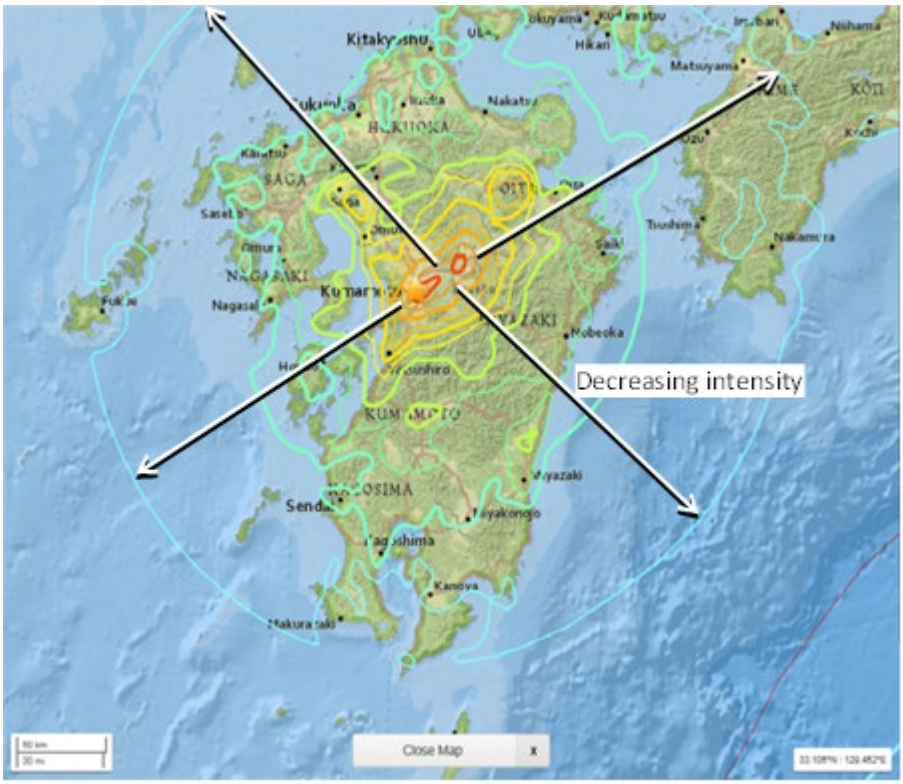

Source: USGS.

Figure 3. Map. Epicentral region of Kumamoto earthquakes, Kyushu.

In terms of lives impacted, the April 14 foreshock resulted in at least 9 fatalities and 1,108 injuries, and the April 16 main shock resulted in 40 fatalities and 2,021 injuries. Many homes in the Kumamoto Prefecture were damaged or destroyed. In addition, reports from Japan described significant damage to highway infrastructure. Immediate investigation by the National Institute for Land and Infrastructure Management (NILIM) and the Public Works Research Institute (PWRI) revealed strong ground motions equivalent to or greater than the ground motions recorded during the January 1995 earthquake near the city of Kobe (population 1.5 million) that killed over 5,000 people. Japan invested heavily in research and development after the Kobe earthquake, resulting in significant changes to seismic design specifications and retrofit procedures. The performance of structures during the Kumamoto earthquakes is particularly significant in that many of the damaged structures had been designed and/or retrofitted to these new standards. Approximately 180 bridges out of 15,000 in the Kumamoto Prefecture were damaged during the earthquakes. This number is relatively low (less than 1.5 percent), given the intensity of the ground motions, and speaks to the validity of the new standards.

Immediate posthazard assessment by NILIM and PWRI reported damage to new bridges even though several had been designed in accordance with the *Design Specifications of Highway Bridges* (Japan Road Association (JRA) 1996). They observed damage to rubber bearings supporting curved steel bridges, hydraulic dampers in an arch bridge, and shear keys; substructure tilting and settlement; and extensive slope failures. U.S. and Japanese researchers and practitioners have a history of collaboration following significant hazard events. The purpose of this collaboration is to learn from the hazards and share knowledge and skills that have benefited both countries as they seek to improve their highway infrastructure. More recently, after the 2011 Great East Japan earthquake and tsunami, information sharing and discussions led to ongoing collaborative research on the tsunami effects on bridges. This collaboration is producing design guidelines vital to the regions of the U.S. Pacific Northwest as well as Japan.

TRANSPORTATION INFRASTRUCTURE RECONNAISSANCE TEAM

Objective

Taking advantage of the opportunity to study the design, retrofit practices, and specifications developed since the 1995 Kobe earthquake, and at the request of the Japanese government, the Federal Highway Administration (FHWA) deployed a Transportation Infrastructure Reconnaissance Team to Japan 3 mo after the earthquakes. Its mission was to conduct post-earthquake assessment on highway bridges in the area affected by the earthquake, examining bridges that performed well and those that failed. A comparative study of the affected infrastructure and the lessons learned could lead to further improvements in design specifications and retrofit procedures to prevent similar damage, increase resilience, and maintain sustainability.

Team Members

FHWA assembled a team of individuals with backgrounds in structural and geotechnical earthquake engineering to form the Transportation Infrastructure Reconnaissance Team. Members were asked to assess bridge performance and compile a report of their findings. The names and affiliations of U.S. and Japanese team members are listed in table 1.

Table 1. U.S. and Japan Reconnaissance Team for the Kumamoto earthquake bridge damage investigation.

Team Member	Affiliation
U.S. side: Sheila Rimal Duwadi, P.E. Principal Research Engineer, Infrastructure Safety and Security sheila.duwadi@dot.gov	 FHWA Turner-Fairbank Highway Research Center 6300 Georgetown Pike McLean, VA 22101
Ian G. Buckle Professor Civil and Environmental Engineering igbuckle@unr.edu	University of Nevada, Reno 1664 N. Virginia Street, Mail Stop 258 Reno, NV 89557-0258
David H. Sanders, P.E. Professor Civil, Construction and Environmental Engineering sandersd@iastate.edu	Iowa State University 813 Bissell Rd Ames, IA 50014
Ron Bromenschenkel Senior Bridge Engineer, Earthquake Engineering Group ron.bromenschenkel@dot.ca.gov	California Department of Transportation P.O. Box 168041, MS 9 2/7J Sacramento, California 95816-8041
Jim Cuthbertson Chief Foundations Engineer, Geotechnical Office CuthbeJ@wsdot.wa.gov	Washington State Department of Transportation P.O. Box 47365 Olympia, WA 98504
Denis Istrati Graduate Research Assistant, Civil Engineering denis.istrati@gmail.com	University of Nevada, Reno 1664 N. Virginia Street, Mail Stop 258 Reno, NV 89557-0258
Japan side: Masahiro Shirato Senior Researcher, Bridge Division shirato-m92ta@nilim.go.jp	 NILIM MLIT, Japan
Jun-ichi Hoshikuma Head, Bridge Division hoshikuma-j92ta@nilim.go.jp	NILIM MLIT, Japan
Shigeki Unjoh Research Coordinator for Earthquake Disaster Prevention unjoh@pwri.go.jp	PWRI Tsukuba, Japan
Nobuhiro Imachou Senior Researcher Earthquake Disaster Management Division	NILIM MLIT, Japan
Yasumoto Aoki Researcher, Center for Advanced Engineering Structural Assessment and Research	PWRI Tsukuba, Japan

MLIT = Ministry of Land, Infrastructure, Transport and Tourism.

Reconnaissance Schedule

The Reconnaissance Team had a full, 3-d schedule in the field. U.S. team members left for Japan on July 10, arrived on July 11, completed their assessment, and returned to the United States on July 14. Visits to the damaged bridge sites were organized by Japanese colleagues at NILIM/PWRI, who provided access to closed areas and greatly facilitated the schedule. The team visited 11 damaged bridge sites with a half-day reserved to discuss of initial findings. The schedule is shown in table 2. A map of the bridge sites visited is shown in figure 4.

Table 2. Schedule.

Date	Destination
July 10–11, 2016 Sunday–Monday	Travel to Japan—United States to Narita then to Fukuoka.
	Lodging in Fukuoka.
July 12, 2016 Tuesday	Visits to the following sites by car and on foot: • Tawarayama Oh-hashi bridge • Susukinohara Oh-hashi bridge • Ooginosaka bridge • Kuwazuru Oh-hashi bridge • Ookirihata Dam bridge • Ookirihata Oh-hashi bridge • Minami Aso bridge • Aso Oh-hashi bridge
	Lodging in Aso area, Kumamoto.
July 13, 2016 Wednesday	Visits to the following sites by car and on foot: • Kiyama River bridge • Akitsugawa bridge • Mashiki Town (epicenter) • Higashibaru bridge
	Fly from Fukuoka to Haneda and then drive to Tsukuba. Lodging in Tsukuba.
July14, 2016 Thursday	FHWA-NILIM meeting in Tsukuba.
	Departure from Narita to the United States.

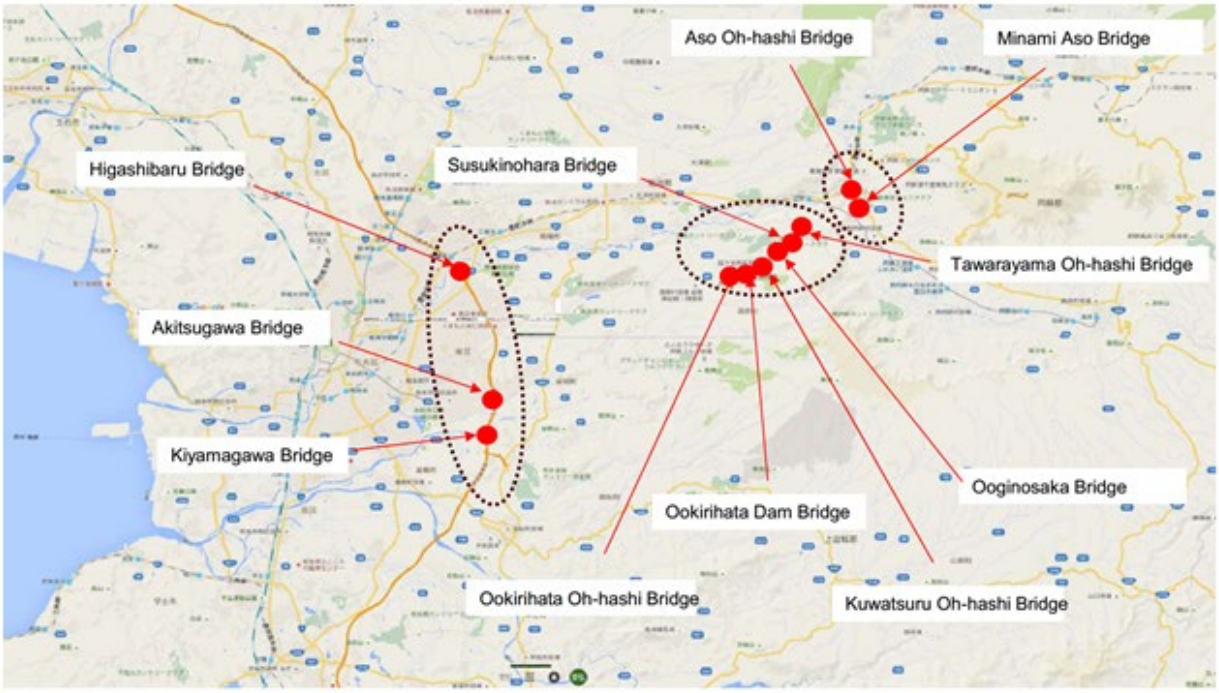

Source: FHWA.

Figure 4. Map. Location of bridges visited by the Reconnaissance Team.

REPORT ORGANIZATION

This report presents reconnaissance findings of earthquake performance of transportation infrastructure based on available information and visual observations. The report is organized to provide, first, an understanding of the geology and seismology of the region and of this earthquake; second, information on the design standards used; and third, observations, lessons learned, and conclusions by the team. Specifically, chapter 2 describes the geology, seismology, and ground motions in and around the Kumamoto area. Chapter 3 reviews the development of seismic design requirements for bridges in Japan. Chapter 4 reports the findings of the Reconnaissance Team related to the performance of new bridges designed to the 1996 specifications and the performance of retrofitted bridges. Chapter 5 summarizes bridge performance and lists lessons learned from the reconnaissance and recommendations.

CHAPTER 2. GEOLOGY, SEISMOLOGY, AND GROUND MOTIONS

BACKGROUND

As noted in chapter 1, the southern Japanese island of Kyushu experienced two significant earthquakes in April 2016. On Thursday, April 14, 2016, a moment magnitude (Mw) 6.2 earthquake occurred NW of the city of Kumamoto in Kumamoto Prefecture at 21:26 JST (Japan Standard Time) (12:26 UTC [Coordinated Universal Time]). Approximately 28 h later, a second larger (Mw 7.0) earthquake occurred beneath Kumamoto early Saturday morning, April 16, 2016, at 01:25 JST (16:25 UTC). Because of the short duration between events, seismologists believe the first event was a foreshock. Having two major earthquakes in the same area resulted in significant structural and property damage, especially in nearby Mashiki Town. The foreshock reportedly caused 9 fatalities and 1,108 injuries in the region, and the main shock caused another 40 fatalities and 2,021 injuries.

The epicenters of the two earthquakes are shown in figure 5 and figure 6.

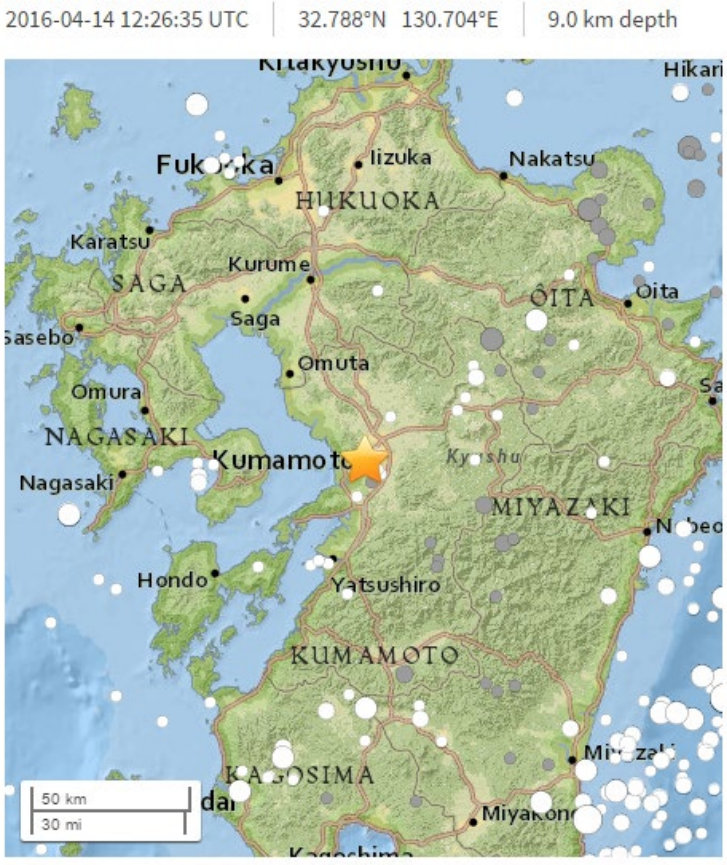

Source: USGS.

Figure 5. Map. Epicenter location of the April 14, 2016, Mw 6.2 Kumamoto earthquake (USGS n.d.).

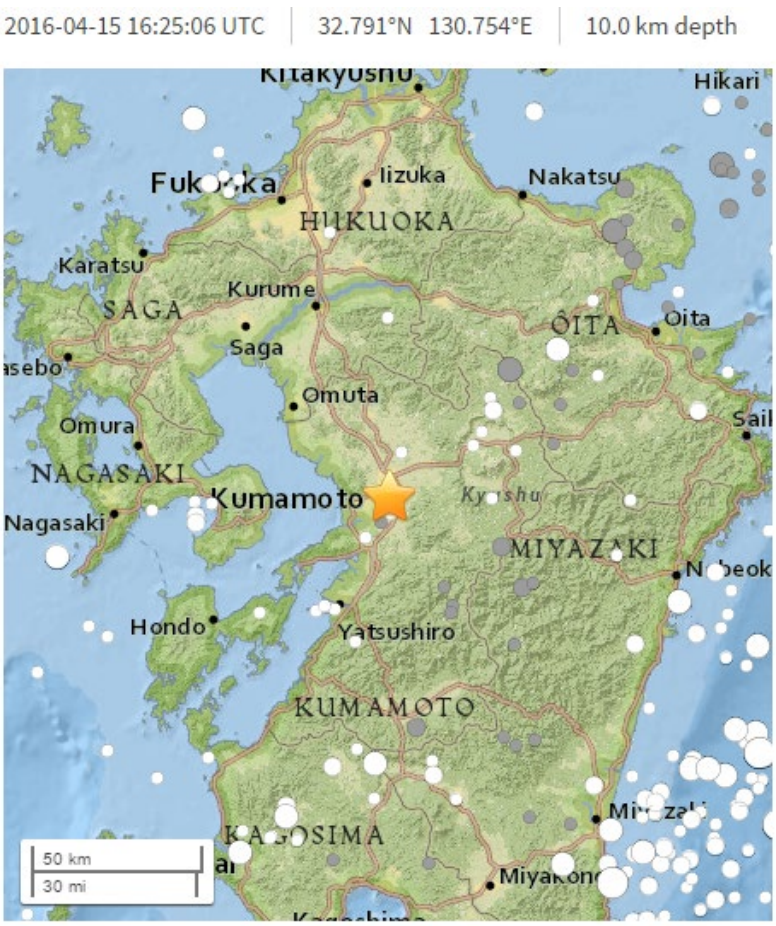

Source: USGS.

Figure 6. Map. Epicenter location of the April 16, 2016, Mw 7.0 Kumamoto earthquake (USGS n.d.).

Several magnitudes have been reported for the two earthquakes. The U.S. Geological Survey (USGS) reports the two earthquakes were Mw 6.2 and Mw 7.0. The NILIM in Japan and the Japan Meteorological Agency (JMA) both reported M6.5 and M7.3. In addition to the magnitude, Japan also uses a seismic scale associated with the level of shaking (shindo) experienced at the ground surface and is similar to the Modified Mercalli scale. The JMA Shindo scale is given in table 3.

Table 3. JMA Shindo scale of earthquake intensity (JMA n.d.).

Seismic Intensity	Human Perception and Reaction	Indoor Situation	Outdoor Situation
0	Imperceptible to people but recorded by seismometers.	—	—
1	Felt slightly by some people keeping quiet in buildings.	—	—
2	Felt by many people keeping quiet in buildings. Some people may be awoken.	Hanging objects such as lamps swing slightly.	—
3	Felt by most people in buildings. Felt by some people walking. Many people are awoken.	Dishes in cupboards may rattle.	Power lines swing slightly.
4	Most people are startled. Felt by most people walking. Most people are awoken.	Hanging objects swing significantly, and dishes in cupboards rattle. Unstable ornaments may fall.	Power lines swing significantly. Those driving vehicles may notice the tremor.
5 Lower	Many people are frightened and feel the need to hold onto something stable.	Hanging objects swing violently. Dishes in cupboards and items on bookshelves fall. Unsecured furniture may move, and unstable furniture may topple over.	In some cases, windows may break and fall. People notice electricity poles moving. Roads may sustain damage.
5 Upper	Many people find it hard to move; walking is difficult without holding onto something stable.	Dishes in cupboards and items on bookshelves are more likely to fall. Televisions may fall from their stands, and unsecured furniture may topple over.	Windows may break and fall, unreinforced concrete block walls may collapse, poorly installed vending machines may topple over, and automobiles and trucks may stop due to difficulty maintaining control.

Seismic Intensity	Human Perception and Reaction	Indoor Situation	Outdoor Situation
6 Lower	It is difficult to remain standing.	Some unsecured furniture moves and may topple over. Doors may become wedged shut.	Wall tiles and windows may sustain damage and fall.
6 Upper	It is impossible to remain standing or move without crawling. People may be thrown into the air.	Most unsecured furniture moves and is more likely to topple over.	Wall tiles and windows are more likely to break and fall. Most unreinforced concrete block walls collapse.
7	It is impossible to remain standing or move without crawling. People may be thrown into the air.	Most unsecured furniture moves and topples over or may even be thrown into the air.	Wall tiles and windows break and fall. Unreinforced concrete block walls collapse.

—No data.

GEOLOGY AND SEISMOLOGY

Tectonic Framework

Japan is on the western Pacific Rim, where the Pacific Plate, PSP, Okhotsk Plate, and Eurasia Plate meet (figure 7).

According to Rhea et al. (2010), in northern Japan, the Pacific Plate is subducting under the Okhotsk Plate into the mantle beneath Hokkaido and northern Honshu. In southeast (SE) Japan, the Pacific Plate is subducting under the PSP and forms the deep offshore Ogasawara and Japan trenches. Along the southern half of Japan and under the island of Kyushu, the PSP is moving NW at a rate of about 2 inches/yr (5 cm/yr), where it subducts under the Eurasia Plate (Wei and Seno 1998).

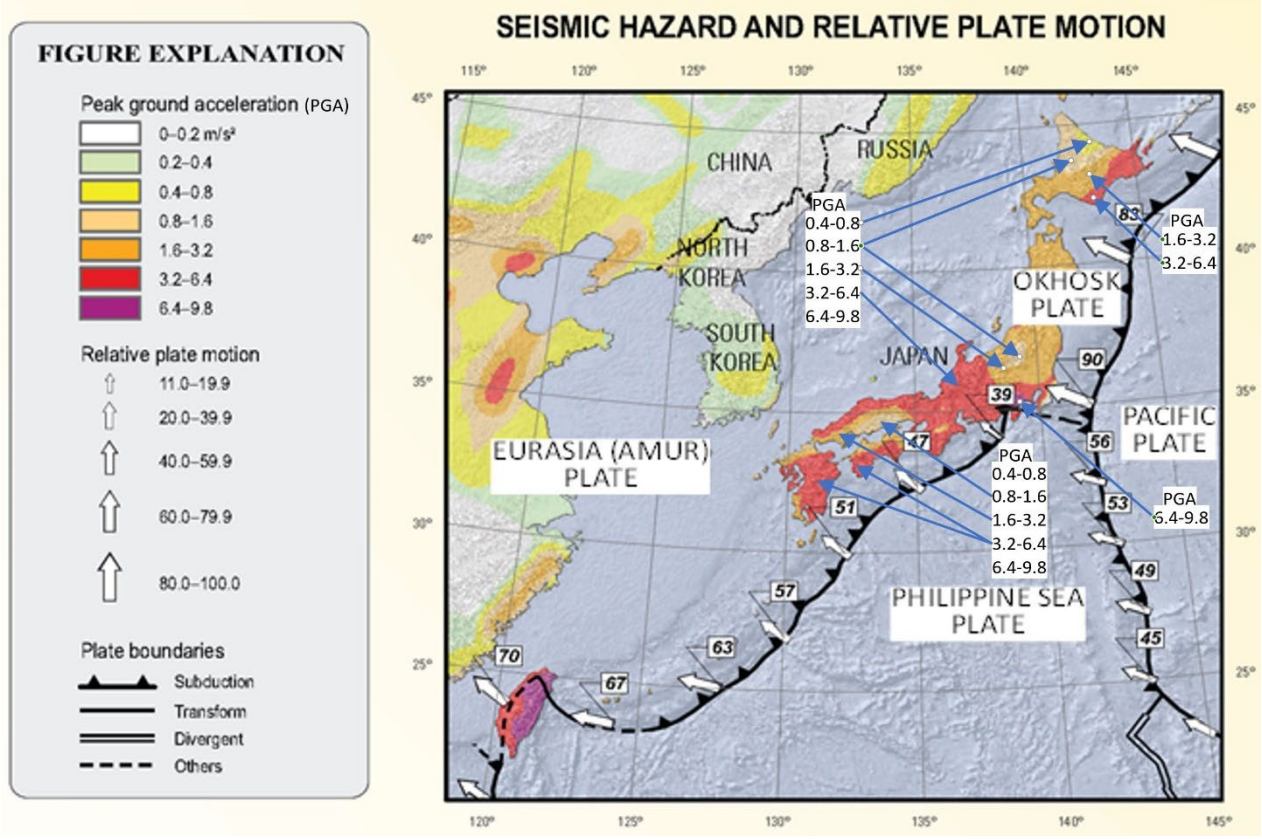

Source: USGS.

Figure 7. Map. Japan's plate structure, relative motion (in millimeters), and seismic hazard (Rhea et al. 2010).

Seismic Source Zones

The subducting PSP under Kyushu highly influences the seismicity and the geology of Kyushu.[1] It causes EW compression and deforms the overriding Eurasia Plate, resulting in faulting, shallow crustal earthquakes, and orogeny. Movement along the subducting plate boundaries causes interplate earthquakes at depths of 25–40 mi (40–60 km). The subducting plate is responsible for volcanism on the island and offshore subduction zone earthquakes with Mw 8.0 and greater. The subducting PSP under Kyushu creates similar conditions to those found along the western coast of the United States. Northern California, Oregon, and Washington have similar plate mechanics, seismic source zones, and volcanism, although Japan is more seismically active than the United States.

Shallow crustal faulting in the Eurasia Plate was the source for the April earthquakes on Kyushu in Kumamoto City and Mashiki Town. Movement occurred on two mapped fault zones: Futagawa and Hinagu (figure 8).

[1]Materials presented by Earthquake Disaster Management Division, 20th FHWA-MLIT Meeting, Tsukuba, July 14, 2016.

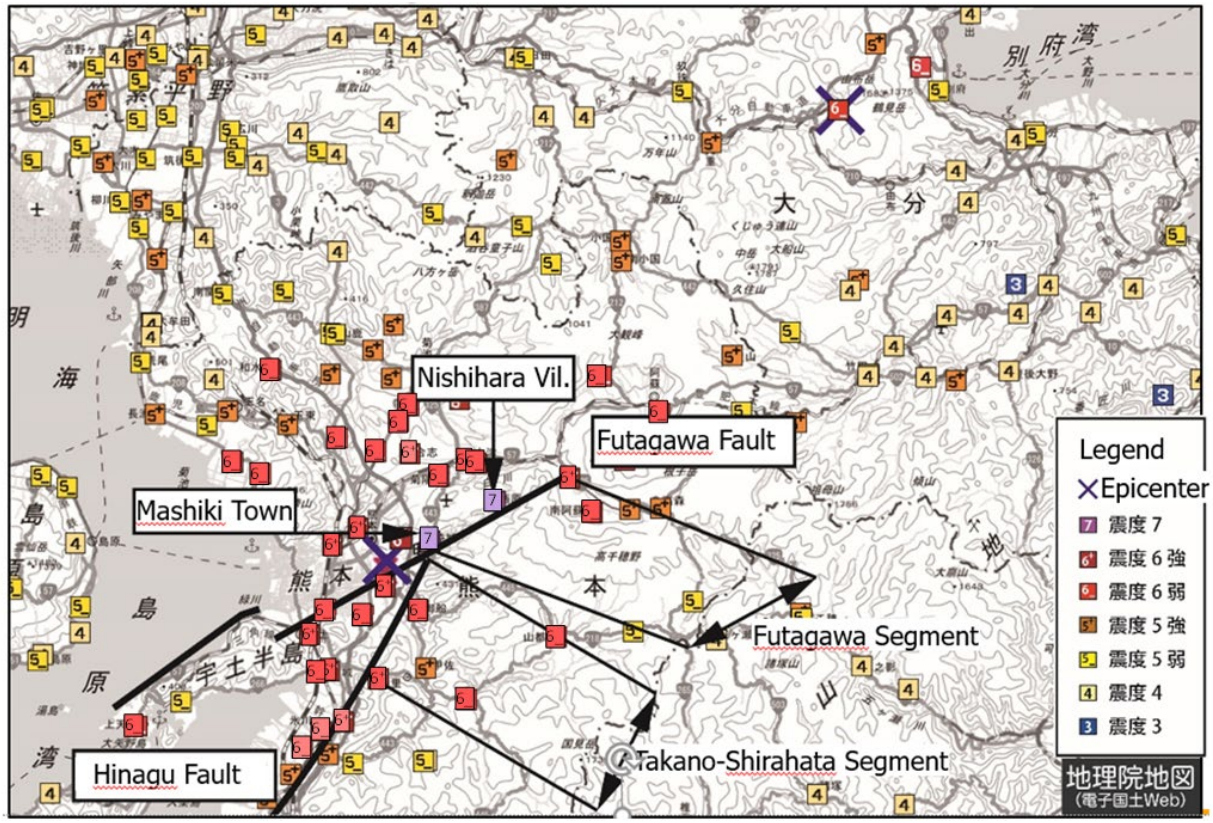

Figure 8. Map. Fault traces in the Kumamoto Prefecture.[2]

Movement along the Hinagu fault was responsible for the Mw 6.2 April 14 earthquake, whereas movement along the Futagawa fault zone was responsible for the Mw 7.0 April 16 earthquake. Both faults are high-angle, right-lateral, strike-slip faults dipping 60–80 degrees.

The Hinagu fault strikes N30°E. During the Mw 6.2 earthquake, the Hinagu fault ruptured along 10 mi (15 km) of its 35-mi (55-km) length, but surface ruptures associated with the April 14 earthquake were not reported (Okumura 2016). Before April, the last reported activity based on paleoseismic study of the Hinagu fault was 2,000–7,400 ^{14}C years before present (yBP), and its vertical displacement amounted to about 10 ft (3 m) (Shimokawa 1999).

Movement on the Futagawa fault was the source of the April 16 Mw 7.0 main shock. This fault is 12 mi (20 km) long and strikes N60°E. Surface ruptures were observed and consisted of a 6-ft (2-m) right lateral permanent offset with about a 3-ft (1-m) vertical subsidence. The last rupture on the Futagawa fault, based on paleoseismic study, occurred earlier than 6,000 ^{14}C yBP (Shimokawa 1999). The April 14 and April 16 earthquakes were not the only earthquakes that occurred between April 14 and 16, 2016. Approximately 140 earthquakes were recorded during this period, and several had JMA seismic intensities greater than 6 (table 4) (JMA 2016).

[2]Ibid.

Table 4. Earthquakes exceeding JMA seismic intensity level 6 since April 14, 2016 (JMA 2016).

Date and Time	Hypocenter	JMA Magnitude	JMA Seismic Intensity
April 14, 2016 21:26 JST (12:26 UTC)	Kumamoto Chiho of Kumamoto Prefecture	6.5[a]	7
April 14, 2016 22:07 JST (13:07 UTC)	Kumamoto Chiho of Kumamoto Prefecture	5.8	6−
April 15, 2016 00:03 JST (April 14, 2016 15:03 UTC)	Kumamoto Chiho of Kumamoto Prefecture	6.4	6+
April 16, 2016 01:25 JST (April 15, 2016 16:25 UTC)	Kumamoto Chiho of Kumamoto Prefecture	7.3[b]	7
April 16, 2016 01:45 JST (April 15, 2016 16:45 UTC)	Kumamoto Chiho of Kumamoto Prefecture	5.9	6−
April 16, 2016 03:55 JST (April 15, 2016 18:55 UTC)	Aso Chiho of Kumamoto Prefecture	5.8	6+
April 16, 2016 09:48 JST (00:48 UTC)	Kumamoto Chiho of Kumamoto Prefecture	5.4	6−

[a] Mw 6.2 USGS.
[b] Mw 7.0 USGS.

Both seismic events produced significant shaking in the Kumamoto area. JMA seismic intensities of 4 were felt throughout the Kumamoto Prefecture. JMA level 4 is characterized by shaking enough to startle people, hanging objects swinging significantly, and dishes rattling in cupboards. Those closest to the epicenters experienced upper level 6 and 7 shaking. These intensities are characterized as follows: it is impossible to remain standing or move without crawling, people may be thrown into the air, most unsecured furniture moves and topples over or may even be thrown into the air, wall tiles and windows are likely to break and fall, and unreinforced concrete block walls may collapse. Figure 9 and figure 10 show the JMA seismic intensities in and around the Kumamoto Prefecture during the foreshock and main shock earthquakes.

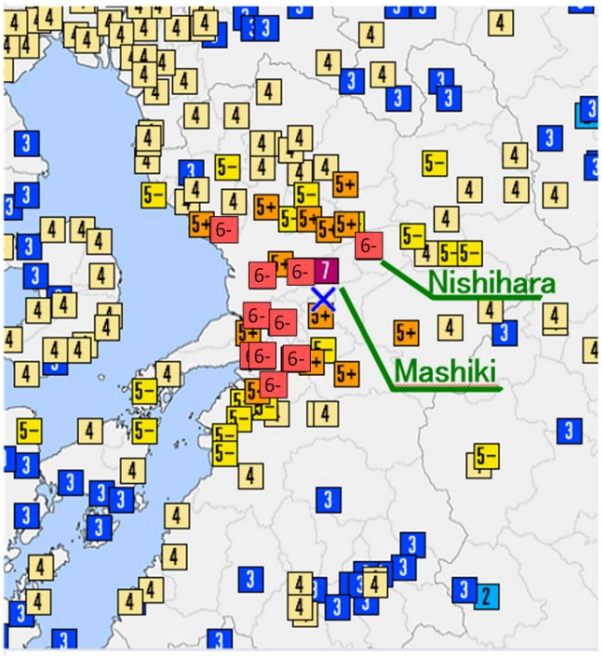

Figure 9. Map. JMA seismic intensity for April 14 Mw 6.2 foreshock.[3]

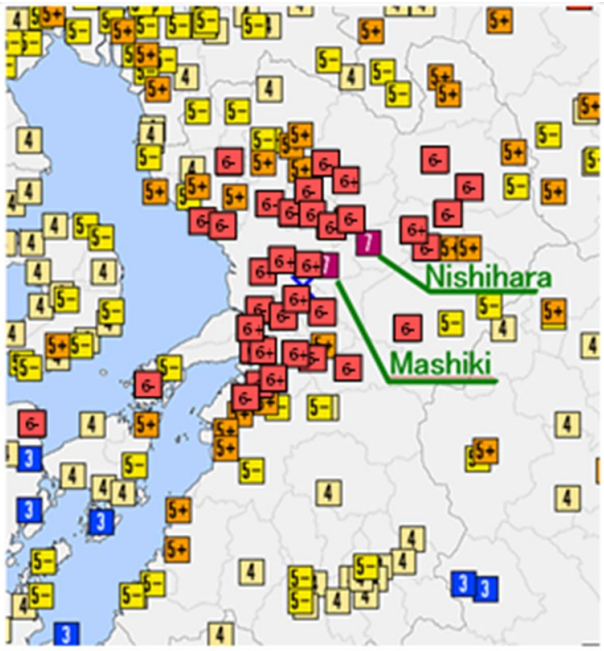

Figure 10. Map. JMA seismic intensity for April 16 Mw 7.0 main shock.[4]

[3]Ibid.
[4]Ibid.

Surface Geology

Some of the oldest basement rock in Japan is Cambrian and Ordovician ophiolites. Younger Jurassic rocks have been accreted onto the Eurasia Plate to form current Japan (Taira 2001). Since the middle Miocene, the predominant geological processes that form modern Japan have been volcanism and weathering. In the area most severely affected by the recent earthquakes, Kumamoto and Mashiki, Holocene alluvium fills the valleys with Pleistocene fluvial terraces and late Pleistocene pyroclastic flows (Okumura 2016). Fine-grained soils of varying plasticity are common in the valleys, as well as deposits of loose, cohesionless sands that are liquefiable.

Ground Motions

Japan has a national seismic network, which has been operated by the National Research Institute for Earth Science and Disaster Resilience (NIED) since June 1996. Japan has two main types of stations: Kyoshin (K-NET) and Kiban Kyoshin (KiK-net). K-NET stations are ground surface seismograph monitoring stations, whereas KiK-net stations are both ground stations and pairs of seismographs installed in boreholes. Table 5 lists the Kumamoto Prefecture stations and their locations. Earthquake motions from these stations can be downloaded from the NIED Strong Motion Seismograph Network website (NIED n.d.).

The accelerograms recorded in Mashiki Town for the foreshock and main shock events can be found in Iwata and Asano (2016). The unit of acceleration used in Japan is the "gal," which is defined as 1 centimeter per second squared (1 cm/s^2). The conversion from gal to gravity is a convenient one: 1 gal = 1 cm/s^2 = 0.001020 *g* = 0.001 *g* (approximately). Accordingly, the peak acceleration for the EW component of Mashiki Town foreshock accelerogram was 732 gal or 0.73 *g* (approximately). The peak acceleration for the EW component of Mashiki Town main shock accelerogram was 825 gal or 0.82 *g* (approximately). Both accelerations are the highest Japan has experienced since the offshore Miyagi earthquake of April 7, 2011.

The subducting PSP causes EW compression in Kyushu. The Futagawa and Hinagu faults strike NE. Therefore, it is not surprising that the strongest shaking was in the EW direction for the two events. Because of the NE strike, the north-south (NS) accelerations were also significant at 0.63 *g* and 0.78 *g* for the foreshock and main shock, respectively. Significant vertical acceleration was also recorded: 0.34 *g* for the foreshock and 0.67 *g* for the main shock. The severity of the shaking has been attributed to the shallow epicentral depths of about 6.2 mi (10 km) for the two events.

The main shock caused the most damage and propagated fault rupture to the ground surface. Two seismic stations were closest to the heaviest damage. One was located in Mashiki Town, and the other was in Nishihara Village. Velocity, displacement, and particle displacement histories were determined from the main shock accelerograms by integration for both stations.

Table 5. NIED seismic stations in Kumamoto Prefecture and their locations.

Network	Site Code	Site Name	Latitude	Longitude	Altitude (ft [m])	Depth (ft [m])	Seismograph
K-NET	KMM001	Oguni	33.1208	131.0687	1,417 (432)	—	K-NET02
K-NET	KMM002	Yamaga	33.0185	130.6846	98 (30)	—	K-NET02
K-NET	KMM003	Tamana	32.9336	130.5477	46 (14)	—	K-NET02
K-NET	KMM004	Ichinomiya	32.9320	131.1214	1,824 (556)	—	K-NET11A
K-NET	KMM005	Ohdu	32.8761	130.8774	407 (124)	—	K-NET02
K-NET	KMM006	Kumamoto	32.7934	130.7772	112 (34)	—	K-NET02
K-NET	KMM007	Takamori	32.8267	131.1226	1,798 (548)	—	K-NET02
K-NET	KMM008	Uto	32.6878	130.6582	13 (4)	—	K-NET02
K-NET	KMM009	Yabe	32.6858	130.9856	1,453 (443)	—	K-NET02
K-NET	KMM010	Misumi	32.6136	130.4874	7 (2)	—	K-NET02
K-NET	KMM011	Tomochi	32.6167	130.8652	466 (142)	—	K-NET02
K-NET	KMM012	Yatsushiro	32.5078	130.6024	10 (3)	—	K-NET02
K-NET	KMM013	Tanoura	32.3650	130.5099	10 (3)	—	K-NET02
K-NET	KMM014	Itsuki	32.3961	130.8268	984 (300)	—	K-NET02
K-NET	KMM015	Minamata	32.2161	130.4046	16 (5)	—	K-NET02
K-NET	KMM016	Hitoyoshi	32.1966	130.7757	489 (149)	—	K-NET02
K-NET	KMM017	Taragi	32.2561	130.9257	509 (155)	—	K-NET02
K-NET	KMM018	Ryuhgatake	32.3942	130.3885	10 (3)	—	K-NET02
K-NET	KMM019	Hondo	32.4548	130.1807	23 (7)	—	K-NET02
K-NET	KMM020	Shinwa	32.3636	130.1807	33 (10)	—	K-NET02
K-NET	KMM021	Amakusa	32.3793	129.9997	33 (10)	—	K-NET02
K-NET	KMM022	Ushibuka	32.1945	130.0265	13 (4)	—	K-NET02
KiK-net	KMMH01	Kahoku	33.1089	130.6949	246 (75)	328 (100)	KiK-net06
KiK-net	KMMH02	Oguni	33.1220	131.0629	1,411 (430)	407 (124)	KiK-net06
KiK-net	KMMH03	Kikuchi	32.9984	130.8301	584 (178)	656 (200)	KiK-net06
KiK-net	KMMH04	Aso	32.9514	131.0199	1,558 (475)	417 (127)	KiK-net06
KiK-net	KMMH05	Namino	32.9553	131.2207	2,274 (693)	328 (100)	KiK-net06
KiK-net	KMMH06	Hakusui	32.8114	131.1010	1,614 (492)	364 (111)	KiK-net06
KiK-net	KMMH07	Mitsumi	32.6234	130.5584	72 (22)	984 (300)	KiK-net06
KiK-net	KMMH08	Yabe	32.6501	131.0251	1,476 (450)	338 (103)	KiK-net06

Network	Site Code	Site Name	Latitude	Longitude	Altitude (ft [m])	Depth (ft [m])	Seismograph
KiK-net	KMMH09	Izumi	32.4901	130.9046	1,706 (520)	328 (100)	KiK-net06
KiK-net	KMMH10	Shinwa	32.3151	130.1811	518 (158)	984 (300)	KiK-net06
KiK-net	KMMH11	Ashikita	32.2918	130.5777	328 (100)	984 (300)	KiK-net06
KiK-net	KMMH12	Hitoyoshi	32.2054	130.7371	344 (105)	404 (123)	KiK-net06
KiK-net	KMMH13	Ue	32.2209	130.9096	574 (175)	581 (177)	KiK-net06
KiK-net	KMMH14	Toyono	32.6345	130.7521	230 (70)	361 (110)	KiK-net06
KiK-net	KMMH15	Minamata	32.1704	130.3647	49 (15)	361 (110)	KiK-net06
KiK-net	KMMH16	Mashiki	32.7967	130.8199	180 (55)	827 (252)	KiK-net06
KiK-net	KMMH17	Tamana	32.9873	130.5608	180 (55)	328 (100)	KiK-net06

—No data.

The permanent displacement is quite large at both sites. For Mashiki Town, the integral shows about 4.9 ft (1.5 m) of displacement to the east and about 2.5 ft (0.75 m) of subsidence. For Nishihara Village, the integral shows about 6.6 ft (2 m) of displacement to the east and about 6.6 ft (2 m) of vertical subsidence. The accelerations were also large. The foreshock was essentially equivalent to the current design acceleration response spectra (figure 11 and figure 12). The main shock exceeded the current design spectra in a certain range of structural periods.

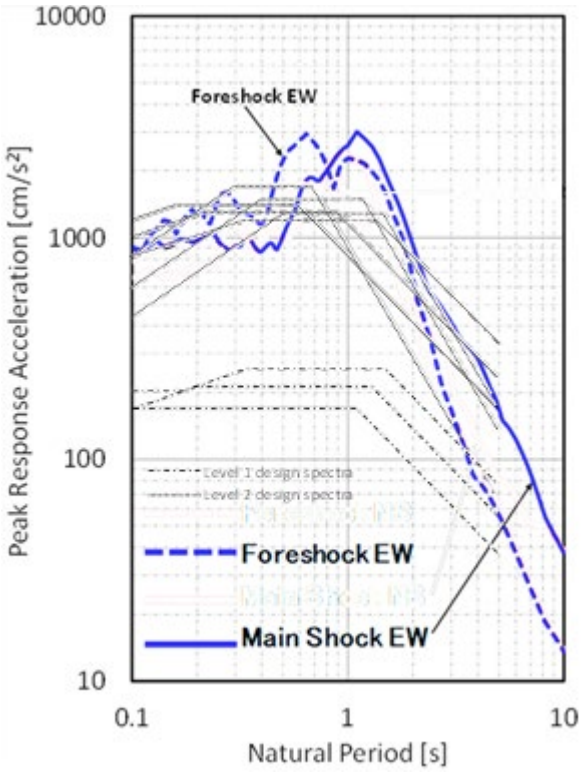

A. EW components.

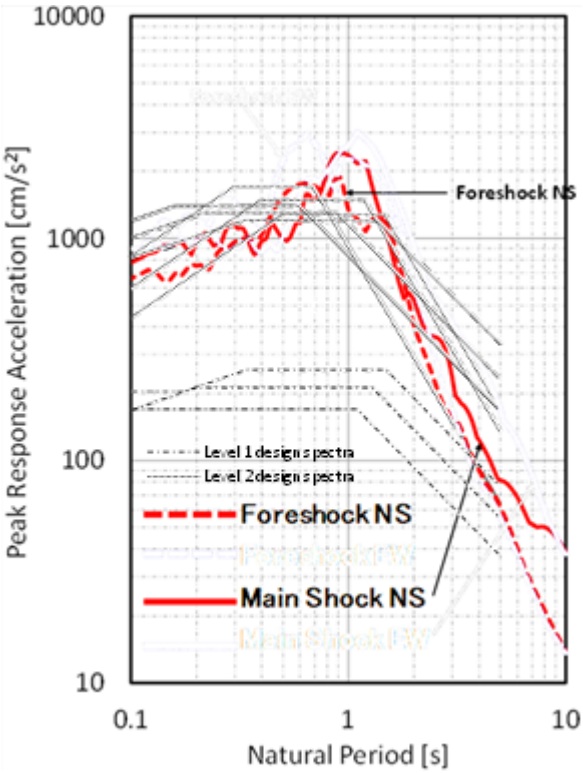

B. NS components.

Figure 11. Graphs. Acceleration response spectra at Mashiki Town for April 16 Mw 7.0 main shock.[5]

[5]Ibid.

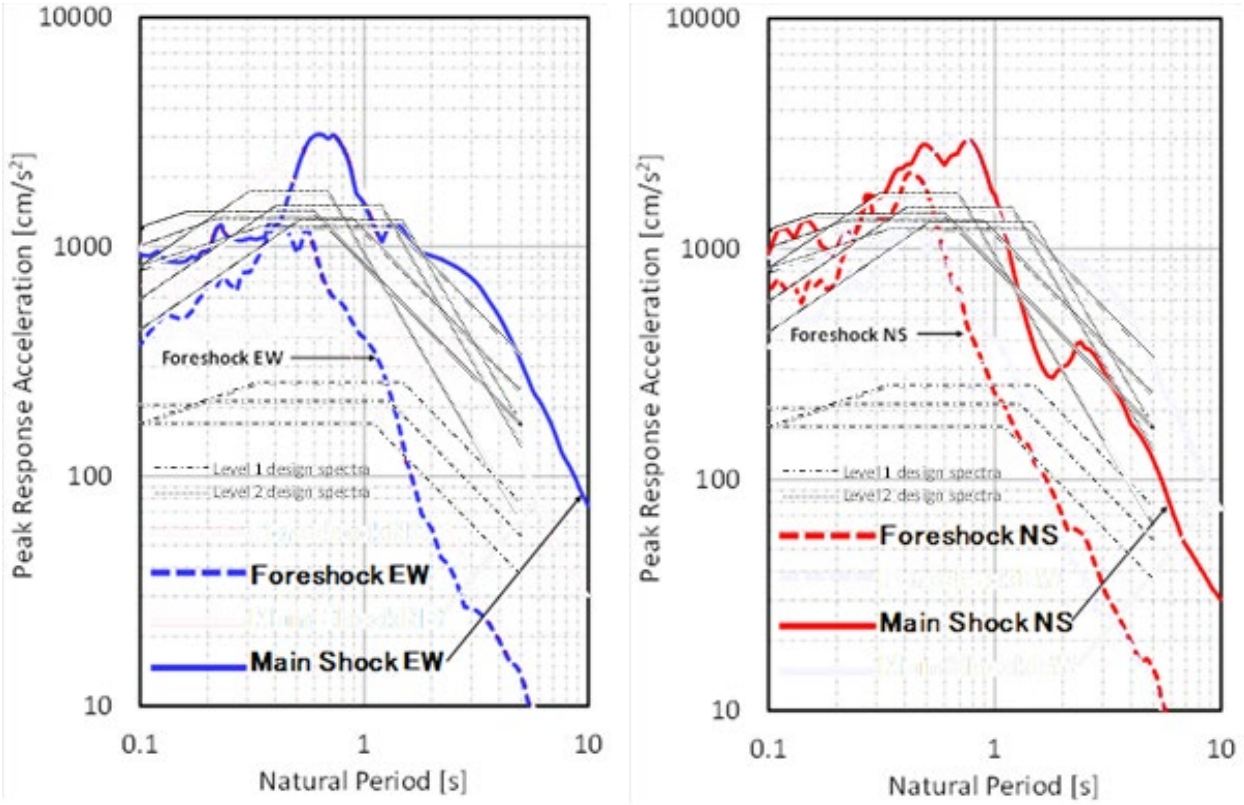

A. EW components.

B. NS components.

Figure 12. Graphs. Acceleration response spectra for Nishihara Village for April 16 Mw 7.0 main shock.[6]

[6]Ibid.

CHAPTER 3. SEISMIC DESIGN REQUIREMENTS FOR BRIDGES IN JAPAN

BACKGROUND

Seismic design methods for highway bridges in Japan have evolved from lessons learned in past earthquakes, going back to the Kanto earthquake (M7.9) of 1923. By introducing various provisions for preventing serious damage, including restrainers to help prevent girder unseating and remediation measures to mitigate soil liquefaction, the number of highway bridges that have suffered complete collapse has been few up until the mid-1990s.

However, the Hyogo-ken-Nanbu (Kobe) earthquake of January 17, 1995, caused destructive damage to many bridges. Collapse or near-collapse of superstructures occurred at 9 locations, and other kinds of major damage occurred at 16 locations (Ministry of Construction 1995; Kawashima 1995). The earthquake revealed a number of critical issues that needed immediate attention in the design and strengthening of bridges for earthquakes.

Immediately after the earthquake, the Committee for Investigation on the Damage of Highway Bridges Caused by the Hyogo-ken-Nanbu Earthquake was established by the Ministry of Construction to survey the damages and investigate their causes. The committee released an intermediate investigative report in March 1995 and a final report in December 1995 (Ministry of Construction 1995). In addition to the investigation of damage, the Committee approved "Guide Specifications for Reconstruction and Repair of Highway Bridges Which Suffered Damage Due to the Hyogo-ken-Nanbu Earthquake" on February 27, 1995, which was immediately adopted by the Ministry of Construction (Kawashima et al. 1996b). Then, on May 25, 1995, the Ministry of Construction announced these guide specifications should be tentatively used throughout Japan as emergency measures for the seismic design of new highway bridges and strengthening of existing bridges, until the *Design Specifications for Highway Bridges* could be revised. This major revision was completed in 1996 (JRA 1996; Kawashima et al. 1996a).

Since then, these design specifications have been continuously improved. A major step was taken in 2002, when performance-based design was introduced to enhance the durability of bridge structures for long-term use, as well as the inclusion of new knowledge about bridge design and performance that had been gained since the 1996 specifications. The 2002 design specifications were issued by the Ministry of Land, Infrastructure and Transport (MLIT) on December 27, 2001 (JRA 2002; Unjoh, Terayama, and JRA 2002).

Following the Great East Japan earthquake of March 2011, another major revision was issued by MLIT on February 16, 2012. The revised specifications and commentary were published in March 2012 (JRA 2012; Kuwabara et al. 2013). These modifications were based on recent research findings in safety, serviceability, and durability of bridges. Examples include the introduction of integral abutment bridges; use of higher strength rebar compared with conventional reinforcement; consideration of age and deterioration on performance; revision of design ground motions for subduction-type earthquakes; and inclusion of requirements to facilitate maintenance, inspection and repair work for bridges. Tsunamis were first mentioned in

the JRA Specification in the 2012 edition (JRA 2012). More information about each revision is given in Kawashima and Unjoh (2004) and Kuwabara et al. (2013).

1996 JRA SEISMIC DESIGN SPECIFICATIONS

Of the damaged bridges that the team visited, five were designed and constructed for the same road realignment in 1998, and their seismic design was based on the same set of provisions, the 1996 JRA specifications (JRA 1996). Accordingly, the changes made in these specifications as a consequence of the Hyogo-ken-Nanbu (Kobe) earthquake of 1995 are of particular interest. These changes are summarized in this section.

Although the damage sustained in the Kobe earthquake was concentrated in bridges designed to older design specifications, making comprehensive revisions to the then current specifications was considered necessary, based on lessons learned, to reduce the extent of bridge damage in future large earthquakes.

Major updates included the following changes (JRA 1996):

- The ground motion of the 1995 Kobe earthquake, which had the largest ground motion to date in terms of its influence on structures, was to be considered for inland, direct-strike-type earthquakes. The Kobe earthquake ground motion was specified as a new design seismic force, in addition to the conventional design seismic forces.

- A ductility design method was introduced, especially for key structural elements such as bridge piers, foundations, bearing supports, and unseating prevention systems, while the traditional seismic coefficient method was retained for conventional design.

- Clarification was added that, to accurately predict the behavior of a bridge during an earthquake, including nonlinear effects in structural members, dynamic analysis was necessary. For this purpose, input earthquake motions were specified, and the provisions concerning analytical models, analytical methods, and safety checks by dynamic analysis were revised.

- Soil layers to be examined and ground motions to be used to evaluate liquefaction potential were specified. A design procedure for the treatment of liquefaction was specified in cases where it would be probable.

- A design procedure was introduced for the treatment of lateral spreading caused by liquefaction under or near a bridge.

- The seismic isolation design method was modified to consider the distribution of seismic force from superstructure to substructures and the increase of damping capacity.

- The stress-strain relationship of concrete in reinforced concrete piers, considering the confining effect of ties and hoops, was introduced. The method of calculating the horizontal force-displacement relationship was revised. Furthermore, a method for evaluating the shear strength of piers considering scale effects, detailed arrangements of

reinforcement to improve the ductility capacity, and a design method for reinforced concrete rigid frame piers based on the ductility design method were also introduced.

- Methods were introduced for calculating the horizontal capacity and ductility of concrete-filled steel piers, as well as seismic design details for hollow steel piers.

- Methods were specified for checking the horizontal capacity and ductility of various types of foundations, including the effects of nonlinearity. A seismic design method for foundations based on the ductility design method was introduced.

- For bearing supports, for which no clear design method has been specified, design seismic forces and design methods were introduced for various types of bearings, including structural design methods for bearing anchorages.

- To reduce the likelihood of span collapse due to girder unseating, the function of restrainers was clarified, and an unseating prevention system was introduced. Design loads and design methods were also specified.

2002 JRA SEISMIC DESIGN SPECIFICATIONS

As noted in 1996 JRA Seismic Design Specifications above, a major step was taken in 2002 when performance-based design was introduced into the design specifications. At the same time, improvements were made based on new knowledge in seismic design.

Major updates included the following changes (JRA 2002):

- Seismic performance criteria for highway bridges were specified to implement the performance-based design concept, along with the determination of design earthquake ground motions and the verification of seismic performance.

- Two-level design criteria were introduced for design earthquake ground motion of moderate intensity with high probability of occurrence, and design earthquake ground motion of high intensity and low probability of occurrence. These criteria in the 1996 JRA specifications were called type 1 and type 2 motions (JRA 1996). In the 2002 update, these motions were renamed level 1 earthquake and level 2 earthquake, respectively. Level 2 earthquakes were further subdivided into interplate, subduction events (type I), and inland shallow events (type II).

- Three seismic performance levels (SPL) were defined and assigned to bridges based on their importance (type A and type B), and earthquake level (level 1 and level 2), as shown in table 6. Expectations with regard to safety, functionality, and reparability for each SPL are shown in table 7.

- Verification methods of seismic performance were reformatted as static analysis and dynamic analysis. The selection of two design methods was clarified. The applicability of the dynamic analysis was greatly expanded, and a detailed verification method based on dynamic analysis was specified.

- Evaluation method for dynamic earth pressure for the level 2 earthquake design was introduced, based on the modified Mononobe-Okabe earth pressure theory. An evaluation method for dynamic water pressure for the level 2 earthquake design was also introduced.

- Verification method for the seismic performance of abutment foundations on liquefiable ground was introduced.

- Evaluation method for the force-displacement models for steel columns with or without infilled concrete was improved.

- Verification method for the seismic performance of steel and concrete superstructures was introduced.

- Evaluation methods for the strength of bearing supports were improved.

- References giving more detail on the design methods and related information were added at the end of the specifications.

Table 6. Seismic performance matrix (Kawashima and Unjoh 2004).

Type of Design Ground Motions	Standard Bridges (Type A)	Important Bridges (Type B)
Level 1 earthquake: ground motions with high probability to occur.	SPL 1: prevent damage.	SPL 1: prevent damage.
Level 2 earthquake: ground motions with low probability to occur. Interplate earthquakes (type I). Inland earthquakes (type II).	SPL 3: prevent critical damage.	SPL 2: limited damage for function recovery.

Table 7. Seismic performance criteria (Kawashima and Unjoh 2004).

SPL	Safety	Functionality	Reparability	
			Short Term	Long Term
SPL 1: prevent damage	Safety against unseating of superstructure	Same functionality as before earthquake	Repair not required to recover functionality	Repair nonstructural damage not affecting functionality
SPL 2: limited damage for function recovery	Safety against unseating of superstructure	Some functionality lost but quickly recovered	Functionality recovered using temporary repairs	Relatively easy to make permanent repairs
SPL 3: prevent critical damage	Safety against unseating of superstructure	—	—	—

—No data.

2012 JRA SEISMIC DESIGN SPECIFICATIONS

As noted in 2002 JRA Seismic Design Specifications section above, another major revision to the design specifications was made following the Great East Japan earthquake of March 2011. These revised specifications were based on lessons learned during this M9 earthquake and tsunami, as well as recent research findings in the safety, serviceability, and durability of bridges. Examples of the revised specifications are as follows:

- Using revised zone factors based on deterministic hazard maps that consider M9 earthquakes and saturation of ground motion intensity. Acceleration spectra were also revised based on new ground motion predictive equations. In addition, a new set of input acceleration response histories for use in response history dynamic analysis was introduced. This set includes nine motions—one for each of three soil classes at each of the three earthquake levels.

- Planning for tsunami inundation and large-scale landslides, introduced for the first time. For example, for the prevention of collapse of important bridges due to extreme tsunami, giving sufficient clearance is recommended to allow the wave to pass under the superstructure.

- Improving the ductility design method to better quantify the ductility capacity of reinforced concrete bridges. In particular, a new equation for plastic hinge length and allowable tensile strain of longitudinal reinforcement that considers the buckling behavior of this reinforcement was introduced.

- Improving requirements for hollow piers to reflect the trend toward thinner walls, higher axial stresses, and rebar congestion. Examples include the requirement that pier sections must be solid in the plastic hinge regions, and haunches must be used at the four internal corners inside the hollow section of the pier.

- Developing seismic design methods for integral abutment and portal frame bridges to take advantage of lower maintenance costs in these types of bridges. Because the abutment backfill is used for earthquake resistance in these bridges, specifications were also developed for soil compaction in the approach embankments, which are more rigorous than those for conventional bridges.

- Using higher strength rebar to reduce congestion in reinforced concrete piers and improve quality of construction. Based on cyclic loading tests of piers, increasing the yield strength from 345 MPa (50 ksi) to 490 MPa (71 ksi) had no adverse effect on minimum bending radius or ductility.

- Including requirements to facilitate inspection, not just for routine maintenance but also for damage surveys following major earthquakes. In addition, consideration is given to facilitate maintenance and repair work, such as:

- Avoidance of designs that will be difficult to inspect and maintain/repair.
- Consideration of maintenance/repair methods and provision of maintenance/repair equipment, such as inspection ladders and walkways.
- Strengthening of girders over abutment and pier seats to facilitate installation of temporary supports and replacement of damaged bearings.
- Preservation of a comprehensive set of bridge records about the investigation, design, construction, quality control, retrofit, maintenance, and repair of every bridge in the inventory.

CHAPTER 4. STRUCTURAL PERFORMANCE OF HIGHWAY BRIDGES

INTRODUCTION

Approximately 180 bridges out of 15,000 in the Kumamoto Prefecture were damaged during the Kumamoto earthquake. This number is relatively low (less than 1.5 percent), given the intensity of the ground motion. The performance of 12 of these bridges is described in this chapter (table 8), including 5 relatively new structures and 5 retrofitted structures. Their approximate locations are given in figure 13, which shows that all but one lie within 1 km of the Futagawa fault.

As shown in table 8, bridge descriptions are grouped in this chapter according to age, as follows:

- Relatively new bridges designed to the 1996 JRA specifications and built in 1999–2000 (JRA 1996).
- Older but retrofitted bridges.
- Other bridges.

Table 8. List of bridges visited and damage sustained.

Bridge Category	Name	Type	Bearings/ Connections Damage	Super-structure Damage	Abutment Damage	Column/ Footing Damage	Ground Failure
A. Recently constructed bridges, i.e., design based on 1996 JRA specifications, as revised after Great Hanshin earthquake (1995), except if noted otherwise (JRA 1996)	Ookirihata Oh-hashi bridge	Curved steel plate girders with concrete columns	●	●	—	●	●
	Ookirihata Dam bridge	Prestressed concrete girders and slab	—	●	—	—	●
	Kuwazuru Oh-hashi bridge (designed to 1994 JRA specifications, but retrofitted) (Japanese Road Association 1994)	Cable-stayed steel tub girders	●	●	—	—	—
	Susukinohara bridge	Concrete girders and slab	—	—	—	—	●
	Tawarayama Oh-hashi bridge	Steel plate girders	●	●	—	—	●
	Ooginosaka bridge	Steel plate girders	●	●	—	—	—
B. Retrofitted bridges	Minami Aso bridge	Steel arch	—	—	●	—	●
	Kiyama River bridge	Steel plate girders on concrete columns	●	●	—	●	—
	Akitsu River bridge	Steel plate girders on concrete columns	●	●	●	—	—
	Higashibaru bridge	Pin-pin columns with external shear keys at abutments	—	—	●	—	—
C. Other bridges	Ookirihata Dam bridge (on old road)	Single-span skew	—	●	—	—	—
	Aso Oh-hashi bridge	Steel arch	●	●	●	●	●

● Visited.
—Not visited.

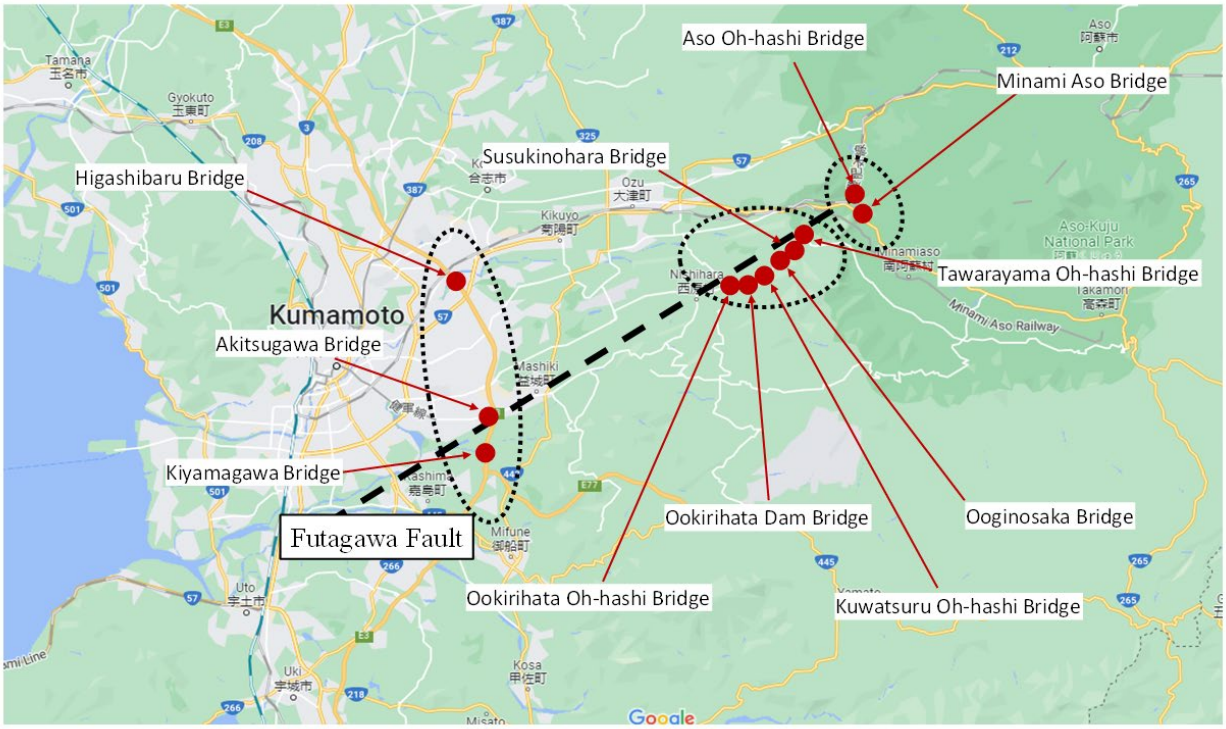

Original Map: © 2022 Google®. Modified by FHWA (see Acknowledgments section).

Figure 13. Map. Location of damaged bridges described in this chapter and proximity to the Futagawa fault.

RECENTLY CONSTRUCTED BRIDGES

In the late 1990s and early 2000s, Route 28 from Mashiki to Takamori in the Kumamoto Prefecture was realigned. This road runs through predominantly hilly country, crossing fast-flowing streams on more than a half-dozen major bridges and through two tunnels. With one exception, all bridges were designed to the 1996 JRA specifications and share many similar details, such as steel plate girder superstructures, concrete deck slabs, and reinforced concrete single-column piers on piled foundations (JRA 1996). All lie within 1 km of the Futagawa fault. The performance of six of these bridges is described in this section.

Ookirihata Oh-hashi Bridge

The Ookirihata Oh-hashi bridge was built in 2001 and is a horizontally curved continuous I-girder steel bridge with five spans and a total length of 871 ft (265.4 m). A pedestrian walkway is located along the north side of the bridge. The bridge is oriented NW-SE.

Abutment A1, which is straight, is in NW, and A2, which is skewed, is in SE, as shown in figure 14 and figure 15. Interestingly, piers P2 and P3 are square (with 11.5 ft (3.5 m) and 13.1 ft (4 m) sides), whereas P1 and P4 are circular. Piers P1 and P4 are supported on deep foundations (shafts) of 14.8 ft (4.5 m) in diameter and 49.2 ft (15.0 m) in length, and 19.7 ft (6.0 m) diameter and 98.4 ft (30 m) length, respectively. Piers P2 and P3 are supported on multiple cast-in-place

piles of 4.9 ft (1.5 m) in diameter with lengths of 45.9 ft (14.0 m) and 42.7 ft (13.0 m), respectively.

Original Map: © 2016 Google®. Modified by NILIM (see Acknowledgments section).

Figure 14. Photo. Aerial view of Ookirihata Oh-hashi bridge and nearby area.[1]

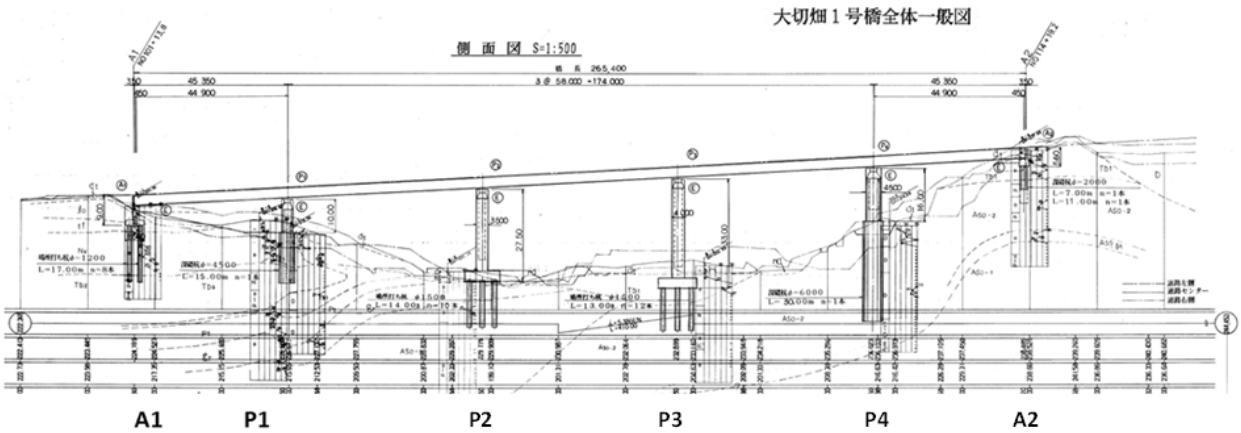

Figure 15. Drawing. Elevation of Ookirihata Oh-hashi bridge.[2]

[1]Materials presented by Earthquake Disaster Management Division, 20th FHWA-MLIT Meeting, Tsukuba, July 14, 2016.
[2]Ibid.

The surrounding area sustained a significant number of slope failures, which damaged a number of retaining walls. A landslide occurred at the location of the bridge, which totally destroyed the adjacent old road (figure 14, figure 16, and figure 17). Only a few retaining walls survived, as shown in figure 18.

Figure 16. Photo. Slope on the south side of the bridge before the earthquake.

Source: FHWA.

Figure 17. Photo. Slope on the south side of the bridge after the earthquake.

Source: FHWA.

Figure 18. Photo. Walls and remnants of the old road on the south side of the bridge.

In addition to the damage in the surrounding area, the earthquake had significant effects on the bridge superstructure and substructure. As shown in figure 19 and figure 20, the superstructure had a large offset toward the north at both abutments, which was approximately 40 inches (1.0 m). This offset was accompanied by extensive failure of the elastomeric bearings. At abutment A1, the bearings below all five girders were ruptured close to either the top plate or the bottom, as shown in figure 21. At the same abutment, some of the longitudinal restrainers failed due to excessive movements of the superstructure (figure 22) from south to north, or due to the combination of lateral and longitudinal displacements that characterize the complex response of a curved bridge. The complexity of the curved bridge response is expected to have been increased by the fact that abutment A2 is skewed. Abrasion on the back wall indicates that pounding of the superstructure on the abutment occurred during shaking (figure 23), which may have led to buckling in the web stiffener under a partial height diaphragm at this abutment (figure 24).

Source: FHWA.

A. North.

Source: FHWA.

B. Measurement of the offset.

Figure 19. Photos. Offset of the superstructure at abutment A1.

Source: FHWA.

A. North.

Source: FHWA.

B. Measurement of the offset.

Figure 20. Photos. Offset of the superstructure at abutment A2.

Source: FHWA.

A. Outside girder G1.

Source: FHWA.

B. Girder G2.

Source: FHWA.

C. Girder G3.

Source: FHWA.

D. Girder G4.

Source: FHWA.

E. Inside girder G5.

Figure 21. Photos. Bearing failure below each girder starting from the outside girder G1 to the inside girder G5 at abutment A1.

Source: FHWA.

A. South.

Source: FHWA.

B. North.

Figure 22. Photos. Rupture of longitudinal restrainers at abutment A1.

Source: FHWA.

Figure 23. Photo. Abrasion on the back wall of abutment A1.

Source: FHWA.

Figure 24. Photo. Damage in girder-to-diaphragm connection at abutment A1.

Apart from the offset of the superstructure at the abutments, significant offsets were also observed at interior piers (figure 25). These offsets were associated with the failure of the connections of the deck to the piers. However, as shown in figure 26 and figure 27, the elastomeric bearings at these locations did not rupture as did those at abutment A1 but, instead, the bolts connecting the top plates to the bearings failed. Pier P2 also had cracking close to the base of the column just above the foundation, indicating the existence of large moments during the shaking (figure 28).

Source: FHWA.

Figure 25. Photo. Offset of superstructure at piers P3 and P4.

Source: FHWA.

A. Side view.

Source: FHWA.

B. Top view.

Figure 26. Photos. Elastomeric bearing at pier P4.

Source: FHWA.

Figure 27. Photo. Elastomeric bearing at pier P1.

Source: FHWA.

Figure 28. Photo. Cracks at the base of pier P2.

Visible damage also occurred at abutment A2 and was primarily at the joints and the bearings, as shown in figure 29, figure 30, and figure 31. At girders G1 and G5, the connections of the elastomeric bearings to their anchor plates seem to have failed. At this same girder, buckling of the stiffener was also observed (figure 31).

Source: FHWA.

A. Overview.

Source: FHWA.

B. Details of the damage.

Figure 29. Photos. Damaged expansion joint at abutment A2.

Source: FHWA.

Figure 30. Photo. Failed bearing below girder G1 at abutment A2.

Source: FHWA.

A. Damaged elastomeric bearing.

Source: FHWA.

B. Damaged stiffener.

Figure 31. Photos. Damage to elastomeric bearing and stiffener at girder G5 at abutment A2.

Ookirihata Dam Bridge

The Ookirihata Dam bridge is a single-span bridge constructed in 1998 with a span of 114.8 ft (35 m). It is a prestressed concrete T-girder bridge on a deep pile foundation with pile diameter of 8.2 ft (2.5 m) and length of 44.3 ft (13.5 m) (figure 32 and figure 33). The ground around the bridge experienced substantial movement, which led to permanent bridge displacement (figure 34 and figure 35).

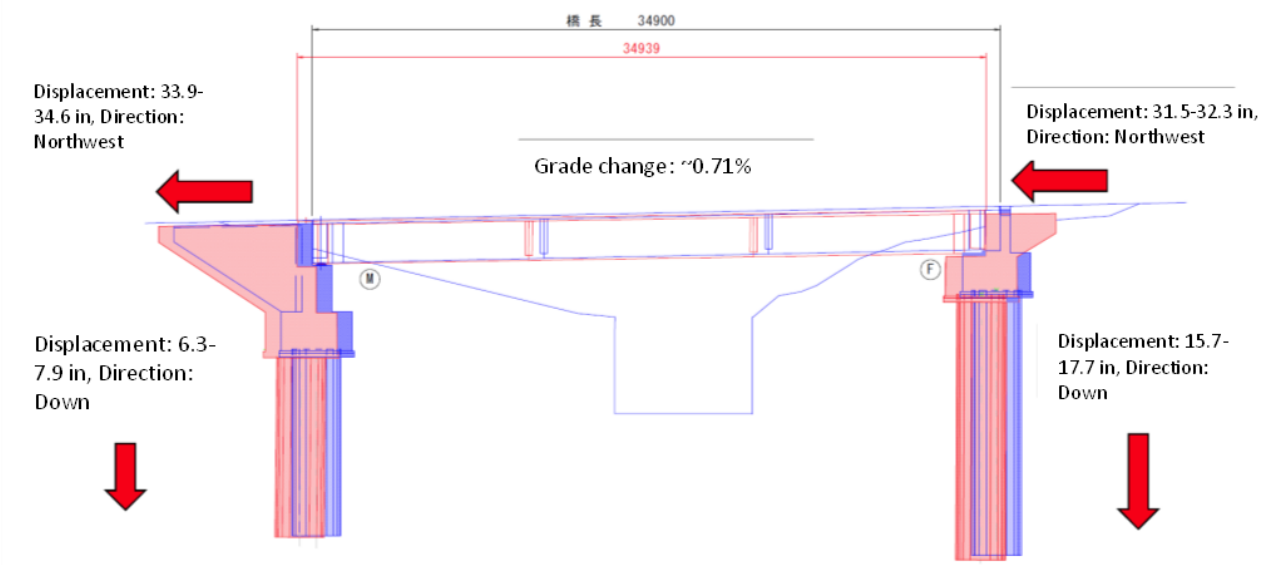

Figure 32. Drawing. Elevation of Ookirihata Dam bridge.[3]

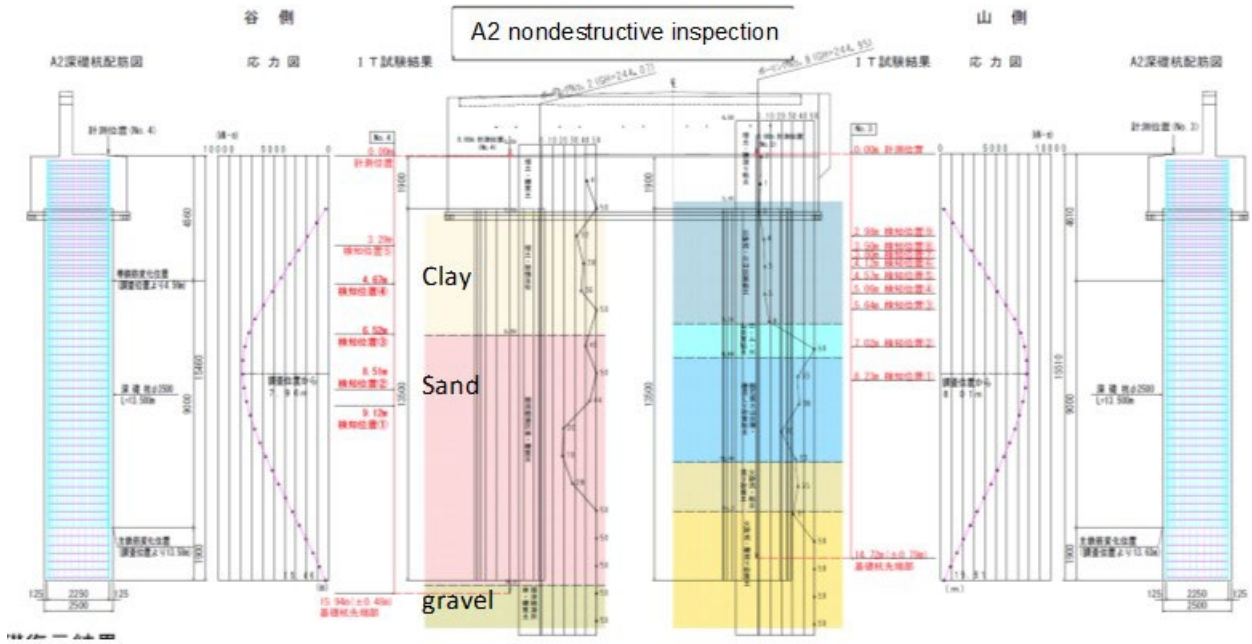

Figure 33. Drawing. Soil profile at the site of Ookirihata Dam bridge.[4]

[3]Ibid.
[4]Ibid.

Source: FHWA.

A. Overview.

Source: FHWA.

B. Measurement of the settlement.

Figure 34. Photos. Approach fill movement at the abutment.

Source: FHWA.

A. Overview.

Source: FHWA.

B. Deformed railing indicating the amount of ground deformation.

Figure 35. Photos. Approach fill movement at the abutment.

Kuwazuru Oh-hashi Bridge

The Kuwazuru Oh-hashi bridge was designed in 1994 and constructed in 1997 following the then-current JRA specifications (figure 36 and figure 37). It was retrofitted based on the specification revisions that occurred following the 1995 Great Hanshin earthquake (Kobe) earthquake. The bridge is oriented south to north, with abutment A1 south and A2 north. It is a cable-stayed bridge with a single central pier consisting of two steel towers that form an "X" in the plane perpendicular to the bridge. The two spans of the bridge are unequal in length. The long span off abutment A1 is 325 ft (99 m), and the short span off abutment A2 is 194 ft (59 m). The short span is 60 percent of the longer span's length. The total structure length is 525 ft (160 m). The superstructure deck has two main steel tub-shaped girders, for the full length, connected by transverse diaphragms. The deck has a 4.8 percent grade, resulting in abutment A2 being 25.3 ft (7.7 m) higher in elevation than abutment A1. The deck has two undivided traffic lanes, one for each direction, with modest shoulders and a multiuse path on one side.

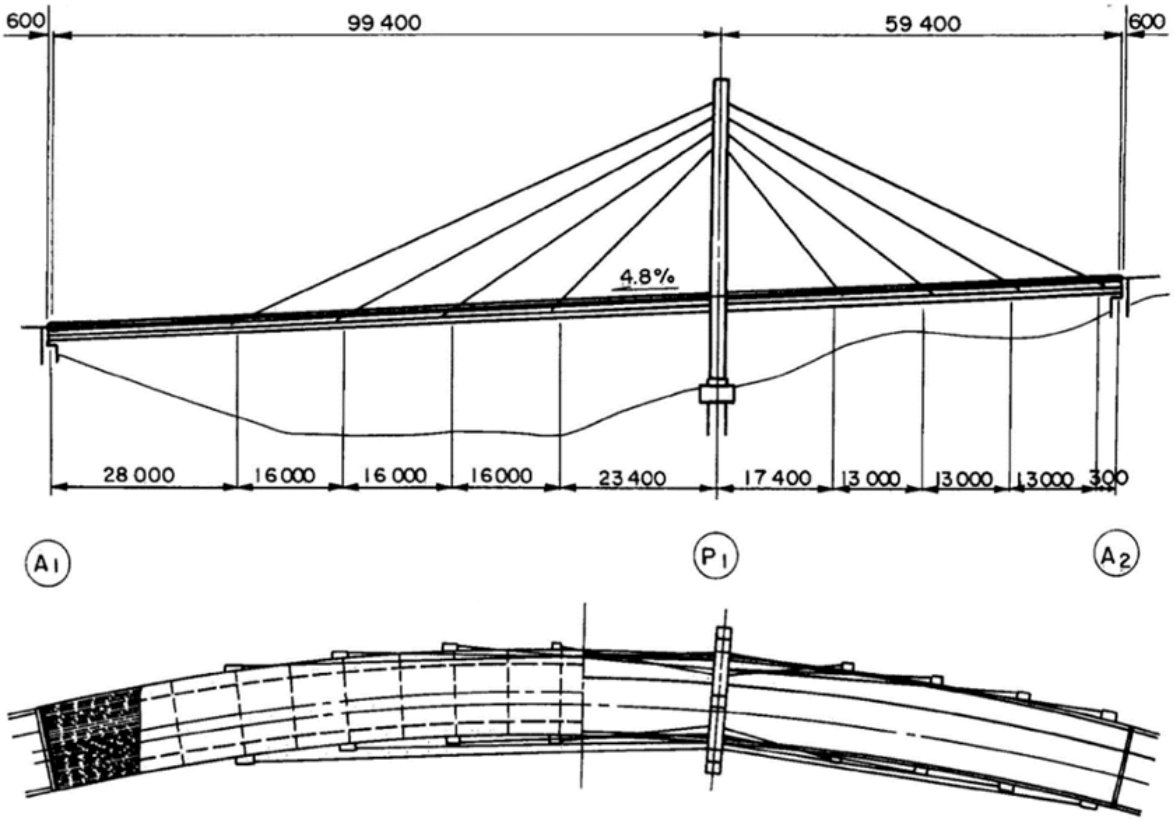

Figure 36. Drawing. Elevation and plan of Kuwazuru Oh-hashi bridge.[5]

[5]Ibid.

Source: FHWA.

Figure 37. Photo. Kuwazuru Oh-hashi bridge looking NE.

There was substantial damage at the abutments. The damage observed at abutment A1 was mainly to the steel bearings and unseating prevention devices (figure 38 and figure 39). The expansion joint at this abutment showed little displacement (figure 40). Abutment A2, which supports the short north span, experienced more damage than abutment A1. The short north span required vertical tension restrainers to maintain its position. These restrainers failed, allowing the superstructure to move upward and lift off the abutment seat. At the same time, the superstructure moved to the right when looking at abutment A2 under the structure. A large arcuate gouge was present in the abutment wall that was lower in elevation than the current girder position, suggesting the gouge occurred on restrainer failure. The steel girder also impacted the stop block and crushed it (figure 41).

Source: FHWA.

A. East bearing.

Source: FHWA.

B. West bearing.

Figure 38. Photos. Damage to steel bearings at abutment A1.

Source: FHWA.

Figure 39. Photo. Damaged restrainers at abutment A1.

Source: FHWA.

Figure 40. Photo. Expansion joint at abutment A1.

Source: FHWA.

Figure 41. Photo. Damage to steel bearings at abutment A2.

At the center pier, the bridge deck was displaced to the west by about 2 ft (0.6 m). Figure 42 shows the superstructure displaced to the west (right side of photo). On the east side of the bridge, the distance to the tower leg is 7.2 ft (2.2 m) at the railing elevation (figure 43). On the west side of the bridge, the distance to the tower leg is 9 inches (23 cm) at the railing elevation (figure 44). The deck was not centered between the tower legs before the earthquake, but the offset is now more severe. Figure 45 shows the damage and permanent displacement of the center pier.

Source: FHWA.

Figure 42. Photo. Center pier of Kuwazuru Oh-hashi bridge.

Source: FHWA.

Figure 43. Photo. Distance from the bridge rail to the east tower leg.

Source: FHWA.

Figure 44. Photo. Distance from the bridge rail to the west tower leg.

Source: FHWA.

A. East side.

Source: FHWA.

B. West side.

Figure 45. Photos. Damage to the east side and west side support blocks at the center pier.

Damage to the cables also occurred (figure 46 and figure 47). On the west side of the long span, a gouge occurred in the high-density polyethylene sheathing on a cable where it appeared to have made contact with a luminaire. The current separation between the luminaire arm and cable appeared to be 3 ft (0.9 m). At least two cables failed, both on the west side of the bridge, one in each span. The failure does not appear to be a complete rupture of the cable and is likely associated with movement of the wedges and anchor plate. This opinion is based on the observed extension in the corrosion protection shielding.

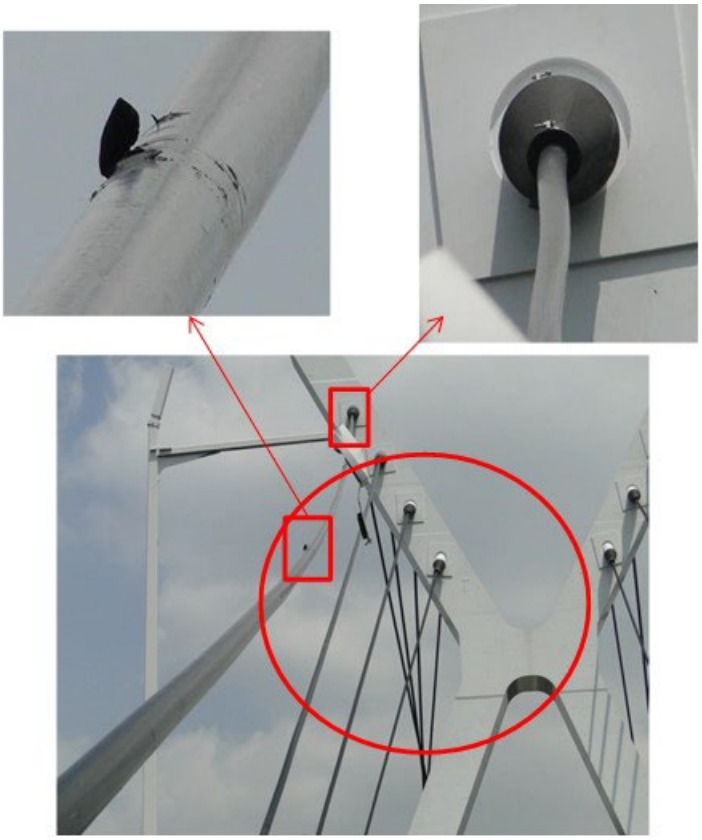

Source: FHWA.

Figure 46. Photo. Cable damage.

Source: FHWA.

Figure 47. Photo. Cable extension.

Susukinohara Bridge

The Susukinohara bridge is oriented EW on Route 28 (figure 48). It was constructed in 1999 and is a 141 ft (43 m), single-span, concrete T-beam bridge. The substructure sits on deep pile foundations bearing on bedrock that is 25–31 ft (7.5–9.5 m) in length. Plan layout and elevation views are shown in figure 49 and figure 50. Although damaged, the bridge survived the earthquake but was closed to traffic.

Figure 48. Map. Location of Susukinohara bridge.[6]

[6]Ibid.

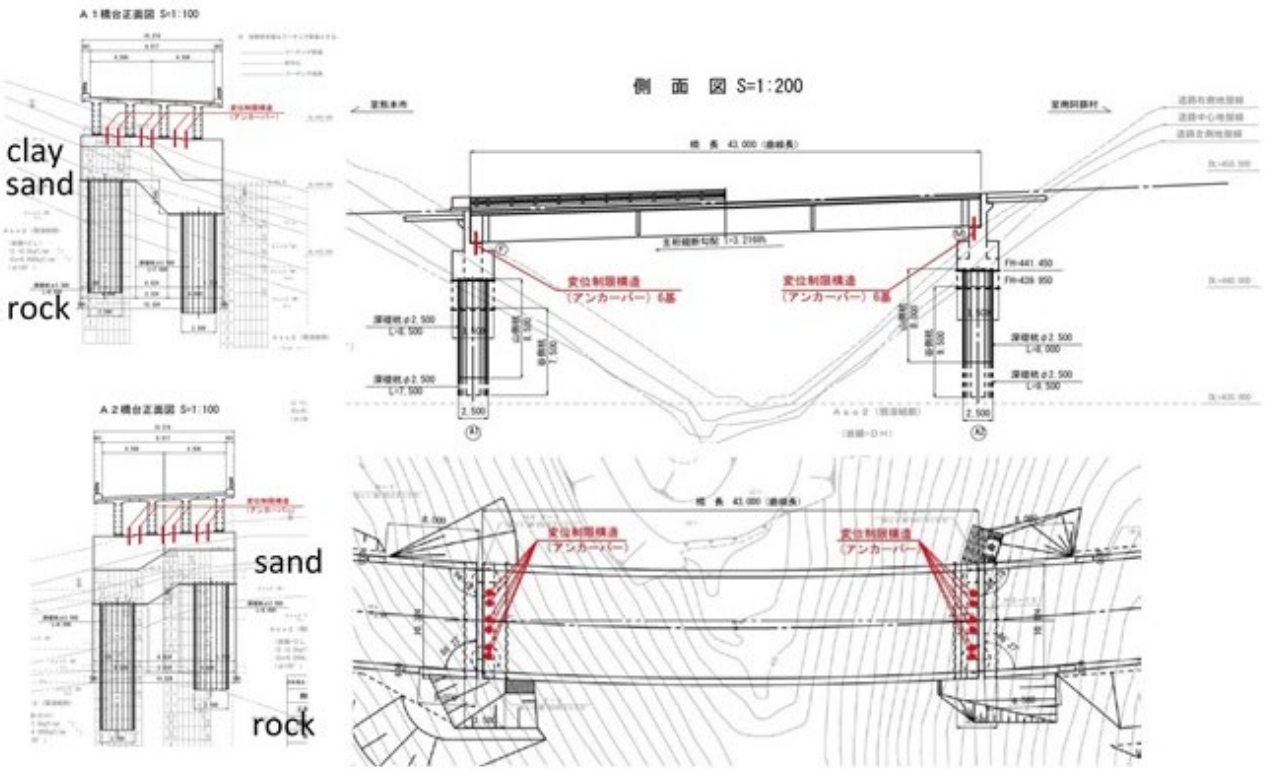

Figure 49. Drawing. Elevation, plan, and cross sections of Susukinohara bridge.[7]

[7]Ibid.

Figure 50. Photo. Susukinohara bridge showing concrete T-girder superstructure with diaphragms.[8]

The damage observed is shown in figure 51, which includes settlement of the bridge relative to the roadway and damage to the end diaphragm at the east abutment due to lateral movement and possible pounding of the girders. No visible cracks were observed on the girders, and, for the most part, there was little damage to the bridge girders or the deck.

[8]Ibid.

Figure 51. Photo. Distant view of damaged approach at the west abutment.[9]

Figure 51 and figure 52 show damage to the approach slab, which had folded up. This damage was at the west abutment. At the east abutment, a large gap appeared between the end of the bridge and the approach (figure 53). This damage indicates the bridge had moved longitudinally toward the west. The amount of permanent lateral movement can be judged from the misalignment of the roadway stripe.

[9]Ibid.

Source: FHWA.

Figure 52. Photo. Close-up view of damaged approach at the west abutment.

Source: FHWA.

Figure 53. Photo. Longitudinal and lateral movement at the east abutment.

Figure 54 shows the rotation of the elastomeric bearing about a vertical axis. However, none of the girders had fallen off the bearings or the abutments. Figure 55 shows timber blocking that is currently being used for additional support.

Figure 54. Photo. Rotation of an elastomeric bearing.[10]

Figure 55. Photo. Timber blocks being used for additional support of girders at abutment seats.[11]

[10]Ibid.
[11]Ibid.

The most severe damage observed in this bridge was the failure of the end diaphragm at the east abutment (figure 56 and figure 57). The longitudinal and lateral movements of the bridge toward the abutment resulted in the failure of the diaphragm.

Source: FHWA.

Figure 56. Photo. Damaged end diaphragm at the east abutment and dislodged timber block from under the second girder from the left.

Source: FHWA.

Figure 57. Photo. Crushing of the end diaphragm at the east abutment.

In summary, the bridge had been displaced both laterally and longitudinally, but there was little damage to the girders or the deck and the riding surface. The damage was mostly to the end

diaphragm and the approaches. The bridge, however, moved permanently out of its original alignment.

Tawarayama Oh-hashi Bridge

The Tawarayama Oh-hashi bridge is oriented EW on Route 28 (figure 58). This three-span, continuous steel, I-girder bridge was constructed in 2001 and has a total span length of 459.3 ft (140.0 m). The cross section consists of three girders with steel cross frames. Finger joints are used for the expansion joints. The bridge is supported on deep pile foundations that are 23–87 ft (7–26.5 m) in length, with soil profile and bridge elevation as given in figure 59. Figure 60 shows the bridge as it sits after the earthquake. It was designed with lateral stoppers on each side of the girders, along with cables to prevent the bridge from lateral and longitudinal movement during earthquakes. It was closed to traffic due to damage.

Figure 58. Map. Location of Tawarayama Oh-hashi bridge.[12]

[12]Ibid.

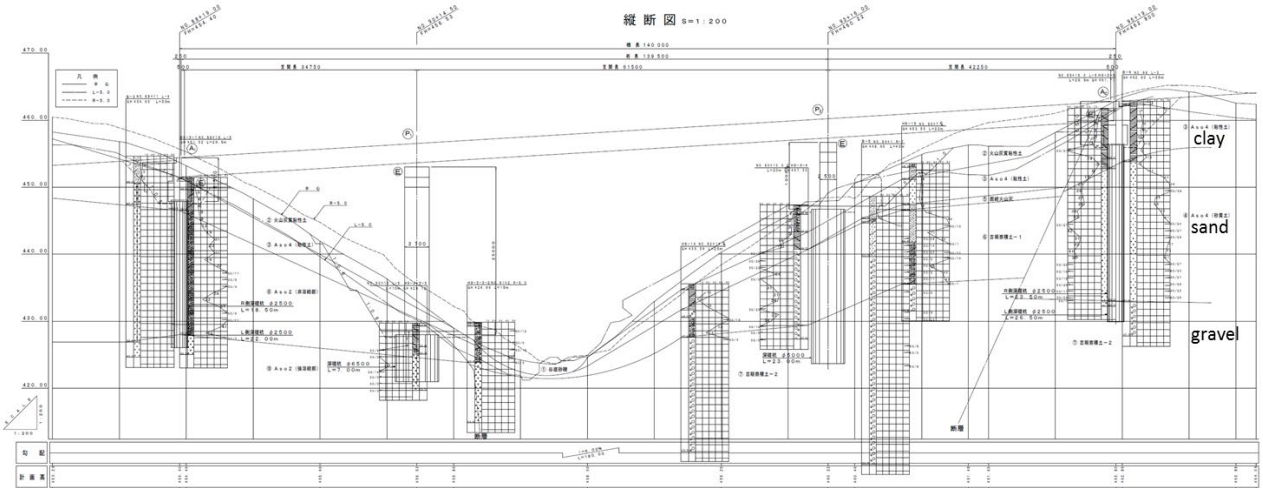

Figure 59. Drawing. Elevation of Tawarayama Oh-hashi bridge.[13]

Source: FHWA.

Figure 60. Photo. Tawarayama Oh-hashi bridge looking east.

The observed damage included girder and cross-frame buckling, bearing distortion, lateral and longitudinal movement of the girders, ground and abutment movement, lateral and vertical movement of finger joints, settlement of approaches, span unseating, shear key failures, and cable restrainer failure. At the road level, settlement of the superstructure and deformation of the railings could be observed. Elastomeric bearings were damaged at several supports.

[13]Ibid.

At the west end, damage was predominantly due to ground movement, leading to failure of the approach roadway, abutment rotation, pounding of girders, and bearing distortion (figure 61, figure 62, and figure 63).

Source: FHWA.

Figure 61. Photo. Failure of the west approach.

All Rights Reserved, Copyright © 2016 National Institute for Land and Infrastructure Management.

Figure 62. Photo. Rotation of the west abutment.[14]

[14]Ibid.

Source: FHWA.

Figure 63. Photo. Pounding at the west abutment and permanent bearing deformation.

Abutment rotation can be visualized in figure 62 from the greater separation distance between the top of the girder and abutment back wall compared with that at the bottom of the girder. Additionally, figure 62 and figure 63 show substantial residual displacement in the bearing. Large permanent displacements in elastomeric bearings were observed on a number of bridges due to residual displacements in their superstructures and/or substructures. Rupture of the drain pipe can also be seen. Furthermore, the back wall was crushed during pounding by the girders, and there was slight distortion of the girders at this location.

In addition to girder distortion at the abutment, buckling was observed in the web and lower flange of the outside girder in the same span (figure 64). This type of buckling failure was not seen in other girders.

Source: FHWA.

Figure 64. Photo. Buckled girder flange and web.

Figure 65 and figure 66 show the condition at the east abutment. As seen in figure 65, the bridge separated from the finger joint and settled about 12 inches (30 cm). Directly below the deck level, figure 66 shows the condition of the elastomeric bearings and the girder. The bearing and the girder moved laterally and longitudinally together and buckled the flange and web as the bridge hit the back wall. This movement resulted in failure of the steel stopper, which was designed to prevent the girder from moving laterally (figure 67).

Source: FHWA.

Figure 65. Photo. Vertical offset at the east abutment between the bridge and approach pavement.

Figure 66. Photo. Lateral movement of a girder and bearing at the east abutment.[15]

[15]Ibid.

Figure 67. Photo. Failure of a bearing stopper at the east abutment.[16]

Additionally, buckling occurred in the lower chord braces (figure 68 and figure 69).

Figure 68. Photo. Out-of-plane buckling of the lower chord brace.[17]

[16]Ibid.
[17]Ibid.

Source: FHWA.

Figure 69. Photo. In-plane buckling of lower chord braces.

Figure 70 shows a typical restraining cable system used to prevent girders from unseating longitudinally. However, as seen in this figure, these cables were not able to prevent lateral movement, as might be expected. Although this restrainer was still attached, the girder moved laterally off the bearing but remained vertical.

Source: FHWA.

Figure 70. Photo. Longitudinal restrainer unable to prevent girder unseating transversely, as might be expected.

Figure 71 shows a close-up view of an elastomeric bearing and the connection details used on the Tawarayama bridge. Four bolts, one at each corner, were used to anchor the bearing to the masonry plate on the abutment seat. Also seen are two transverse stoppers to guide the bearing in the longitudinal direction. All four bolts were sheared off, and the bearing rotated about 90 degrees at this location.

Source: FHWA.

Figure 71. Photo. Elastomeric bearing and transverse stopper at the east abutment showing rotation of the bearing and implied bolt fractures in anchor plates.

Figure 72 and figure 73 show damage at the pier locations. The superstructure as a system moved laterally, distorting the bearing pads on the pier closest to the west abutment (figure 72). On the second pier, shown in figure 73, the superstructure moved off the bearing pads altogether and is sitting directly on the pier. This movement is about 3 ft (about 1 m). Spalling of the concrete is also present on the pier cap, possibly due to the impact of girders falling from the bearings onto the cap.

Source: FHWA.

Figure 72. Photo. Permanent deformation in the elastomeric bearing on pier P1.

Figure 73. Photo. Permanent lateral movement of the superstructure and girder unseating on pier P2.[18]

[18]Ibid.

Figure 74 shows a bracing detail in the plane of the lower flange that was not damaged. This lack of damage was also noted in other bridges on Route 28. Despite strong ground shaking and pervasive ground failures, many superstructure details performed very well.

Figure 74. Photo. Undamaged connection detail for lower chord bracing.[19]

In summary, although the Tawarayama Oh-hashi bridge was out of alignment after the earthquake, and many bearings were damaged as a result, no span collapsed, thus satisfying the life-safety performance criterion.

Ooginosaka Bridge

One of the larger bridges in this group on Route 28, the Ooginosaka bridge is a five plate-girder bridge consisting of two equal 127.6-ft (38.9-m) end spans and a 160.1-ft (48.8-m) center span. The superstructure is supported by tall reinforced concrete columns on large shaft foundations. Constructed in 2000, it is built on a slight horizontal curve and is oriented primarily in the NS direction. A pedestrian walkway/bike path is located along the west side of the bridge. Visible damage was primarily to the bearings, shear keys, and joints. A subsurface investigation to discover possible foundation damage was underway at the time of the reconnaissance.

The nature of superstructure and substructure movement was of most interest. Figure 75 shows a seemingly westerly shift of the superstructure relative to its abutment. Figure 76 shows the relocking of finger joints, indicating the bridge moved longitudinally enough to open the joint, shifted, and closed again in a new offset position. The south end shift was approximately 12 inches (0.30 m). Examining the north abutment (figure 77) revealed a 10-inch (0.25-m) easterly shift. This shift suggests a clockwise rotation of the superstructure (figure 78. However, the at-rest position of the intermediate bearings indicates another possibility. Instead of having slightly less displacement of the same direction as the nearest abutment (with rotation about the

[19]Ibid.

center of the structure), the intermediate bearings were set in opposite directions. Figure 79 shows the easterly offset of the superstructure at the second support and the westerly offset at the third.

Source: FHWA.

Figure 75. Photo. Ooginosaka bridge from the south approach showing left lateral offset at the abutment.

Source: FHWA.

Figure 76. Photo. Finger joint relocking.

Source: FHWA.

Figure 77. Photo. North abutment with easterly superstructure shift.

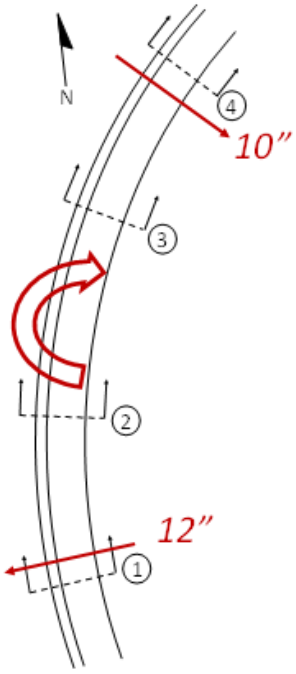

Source: FHWA.

Figure 78. Illustration. Potential rotation of superstructure creating observed abutment offsets.

Source: FHWA.

A. Pier P2.

Source: FHWA.

B. Pier P3.

Figure 79. Photos. Offset at the pier cap for piers P2 and P3.

If these movements are entirely caused by superstructure movement, there must be significant in-plane deformation for the deck, which would produce significant cracking. That was not the case. The deck condition indicated that the deck remained a rigid diaphragm. Figure 80 shows the

direction of movement of each substructure that would have produced the bearing offsets. This result means the ground supporting each foundation through the canyon moved in the opposite direction relative to the next foundation. Given the amount of slope instability in the region, this is a conceivable conclusion. One way to check this concept is to view the center supports from each abutment and check for column drift. Aside from construction tolerances, columns that are out of plumb may indicate seismic shifts in local supporting soil and foundations. When one looks south along the column edges from under the north abutment, the column drifts become evident as a gap can be seen between the tops of the columns in figure 81. A corresponding lower gap can also be seen when one looks north from the southerly abutment (figure 82). Other damage at the bridge included failed shear keys. Figure 83 shows the south abutment shear key after being hit by its steel bumper. Keys were located only in the outside direction of transverse travel, as movement to the east would be less due to the geometry of the inside of the curve.

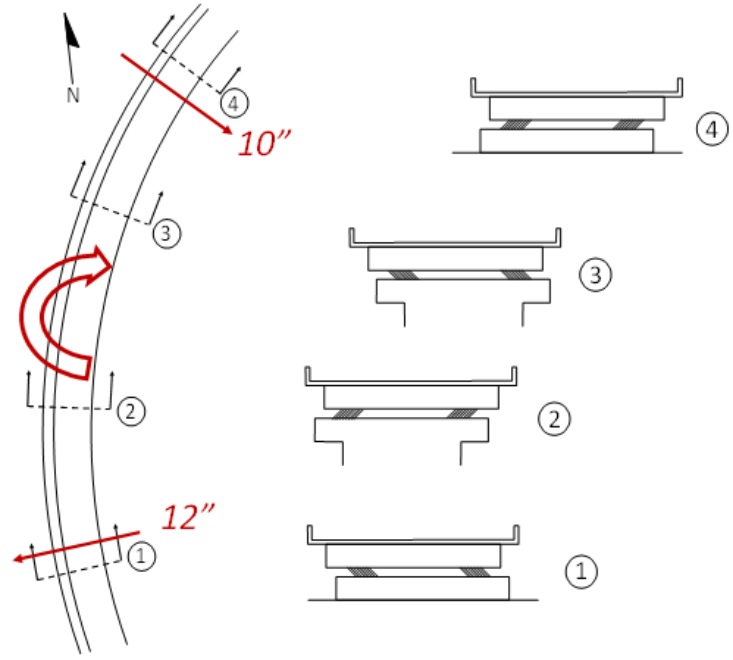

Source: FHWA.

Figure 80. Illustration. Directions of substructure movement necessary to explain observed bearing displacements at each location.

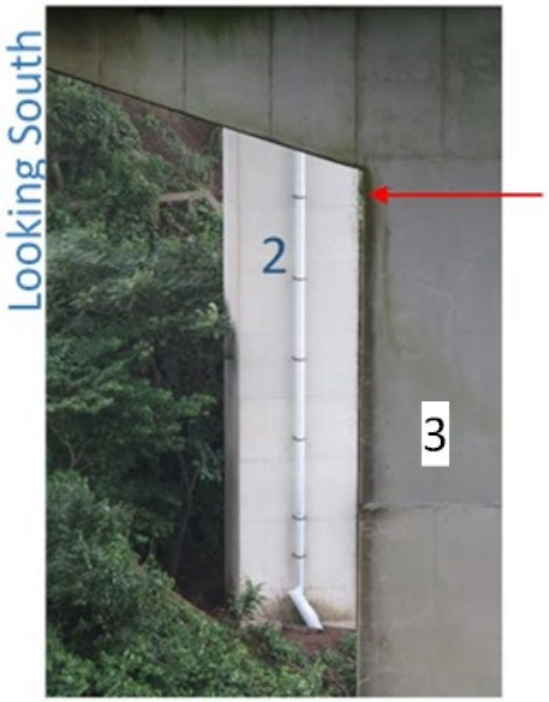

Source: FHWA.

Figure 81. Photo. Gap at the top of superposed column profiles, looking south.

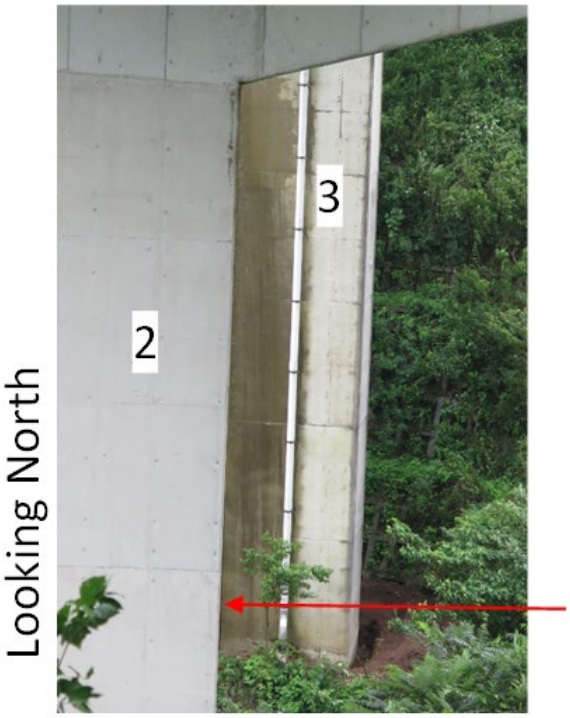

Source: FHWA.

Figure 82. Photo. Gap at the bottom of superposed column profiles, looking north.

Source: FHWA.

Figure 83. Photo. South abutment shear key damage.

Retrofitted Bridges

Japan has an active seismic retrofit program, and practically all bridges on the national expressways and major highways have been retrofitted. The performance of five of these structures is described in this section.

Minami Aso Bridge

This structure comprises a steel arch for the main span and two short back spans for a total length of 364 ft (110.8 m). Built in 1971, the bridge is located on national Route 325. It had been retrofitted using longitudinal dampers at both abutments and buckling-restrained braces in the transverse frames directly above the springing blocks. Figure 84 shows the west side of the structure looking north.

Source: FHWA.

Figure 84. Photo. West side of Minami Aso bridge viewed from the south abutment wing wall.

Damage was primarily sustained by the shear keys and back walls at both abutments. Figure 85 and figure 86 show close-ups of shear key failures at both sides of the south abutment. Dampers were secured to the abutments in the upper shear key area. Transverse displacements at the south abutment appear to have broken the keys, rendering the dampers ineffective. Another possible failure scenario is that longitudinal forces in the dampers pulled the keys free and damaged the back wall, but there was no evidence of longitudinal movement in the road joints at either end of the bridge or of damage to the dampers (no oil leakage, mounting bolt yielding, or pin distortion). A more likely scenario is first the transverse failure of shear keys and then anchorage failures in the dampers due to the weakened back wall. This hypothesis is consistent with the angle of the failure plane in the keys as seen in figure 88 and figure 89.

Source: FHWA.

Figure 85. Photo. Damage to the anchorage of longitudinal damper and shear key on the west side of the south abutment.

Source: FHWA.

Figure 86. Photo. Damage to the anchorage of the longitudinal damper and shear key on the east side of the south abutment.

Dampers were still secured at the north abutments. However, shear cracks at both keys were visible (figure 87, figure 88, and figure 89), indicating a high level of transverse demand.

Source: FHWA.

Figure 87. Photo. Longitudinal damper on the east side of the north abutment.

Source: FHWA.

Figure 88. Photo. Damage to the shear key block on the east side of the north abutment.

Source: FHWA.

Figure 89. Photo. Damage to the shear key block on the west side of the north abutment.

Note the longitudinal bumpers mounted below the bottom girder flanges in figure 87 and figure 89. It is likely these bumpers were designed to prevent dampers from bottoming out in a compression cycle, further supporting the failure sequence in which the keys failed first. All chain restrainers appeared undamaged.

Kiyama River Bridge

The Kiyama River bridge is located in Kumamoto Prefecture and is part of the Kyushu Expressway (figure 13). It is a composite bridge with four steel girders and cross frames. This structure was built in 1976 and has 32 spans, including a number of two-span and three-span continuous segments. It has a total length of 2,844 ft (867.0 m). The bridge runs NS and has a small in-plane curvature. The piers are supported on pipe piles 95–130 ft (29–40 m) long, which are either vertical or battered, as shown in figure 90. There are actually two parallel bridges, one for each direction of traffic, as shown in figure 91. Between 2005 and 2007, the bridge was retrofitted using concrete jackets for the columns and unseating prevention devices at certain supports. However, the girders, bearings, pier-to-pile cap connections, and foundations were not retrofitted at that time.

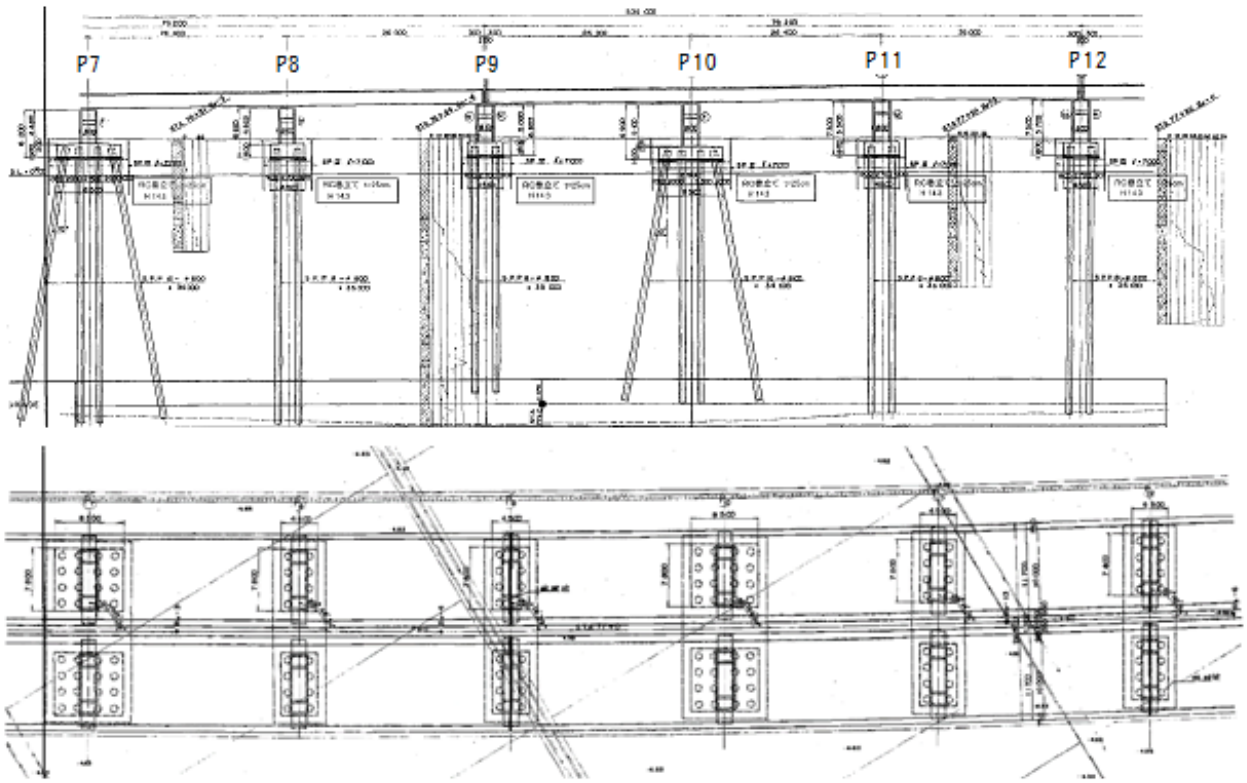

Figure 90. Drawing. Elevation and plan of Kiyama River bridge from pier P7 to pier P12 (NILIM 2017).

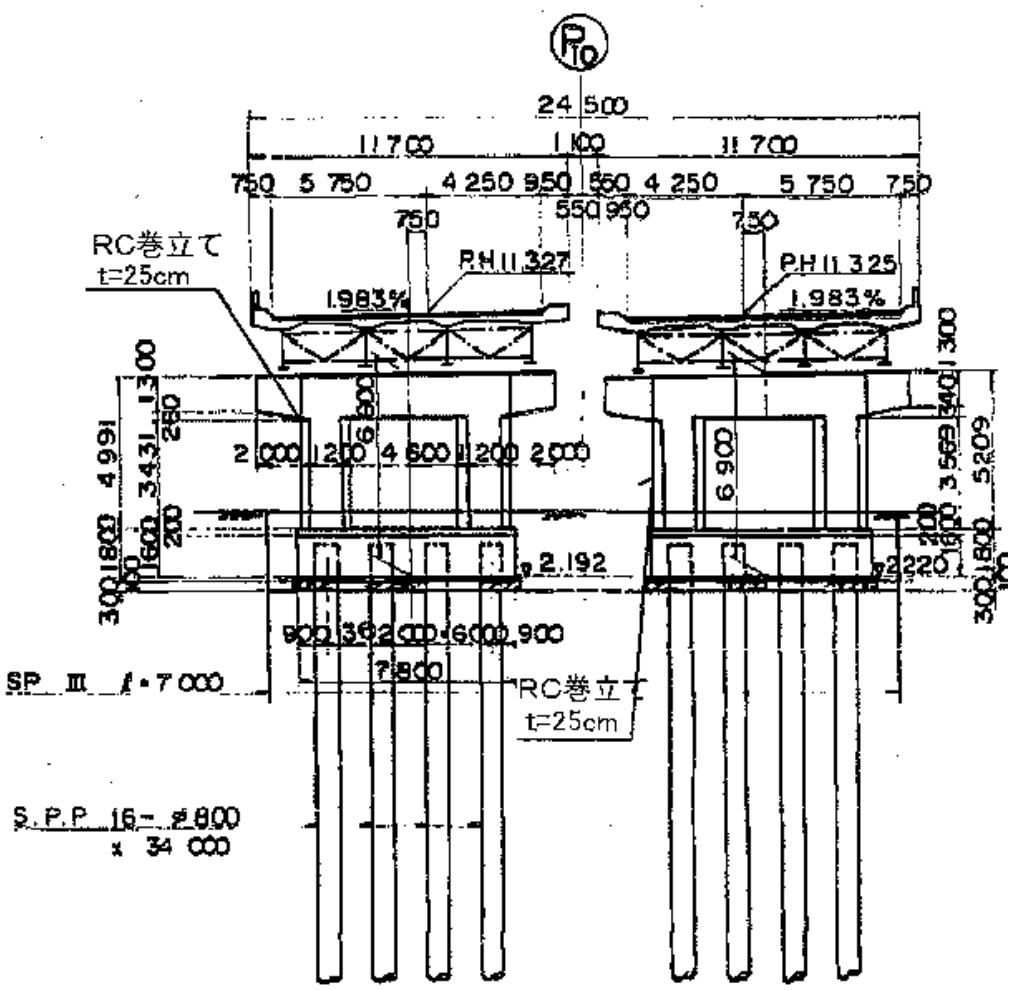

Figure 91. Drawing. Cross section through the east and west bridges from pier P7 to pier P12 (NILIM 2017).

During the Kumamoto earthquake, the eastern bridge moved to the north and east. This movement resulted in the opening of a gap at pier 12 (figure 92) and the misalignment of consecutive spans (figure 93) in the eastern bridge. According to NEXCO West Japan—the company that manages the bridge—the western bridge shifted during the foreshock but then shifted back in the main shock. The heavy damage to the eastern bridge rendered it nonoperational, and it was closed to traffic, but the western bridge remained open.

Source: FHWA.

Figure 92. Photo. Opening of the expansion joint at pier P12 of the east bridge.

Source: FHWA.

Figure 93. Photo. Misalignment of consecutive spans at pier P12 of the east bridge.

As shown in figure 90, the three piers, P10, P11, and P12, supported a two-span continuous segment with expansion joints at each end. This segment is the one that shifted east by approximately 3 ft (1 m), and the misalignment is observed at the joints of P10 and P12. At the time of the visit of the Reconnaissance Team, falsework and temporary supports had been installed below the segment in order to lift the deck and move it back to its initial position (figure 94).

Source: FHWA.

A. Span-end support.

Source: FHWA.

B. In-span support.

Figure 94. Photos. Temporary support systems at pier P12 of the east bridge.

Pier 11 of the east bridge was the only pier reported to have extensive damage. It was also the only pier on which the anchorages of the pinned bearings on the cap beam had not failed, thus, subjecting the pier to significant longitudinal load from the superstructure. The rotation can be seen in figure 95. It opened a vertical gap of about 2.5 inches (6.35 cm) between the column jacket and pile cap, which seemed to run the entire length of the cap. It was observed under both columns of pier P11 of the eastern bridge, indicating the reinforcement connecting the column to the pile cap had been either yielded, pulled out, or sheared. It was not possible to be more definitive without demolishing the column. This damage is shown in figure 96, figure 97, and figure 98.

Source: FHWA.

Figure 95. Photo. Side view of tilted pier P11.

Source: FHWA.

A. Overview of the pier.

Source: FHWA.

B. Close-up for the column-pile cap connection.

Figure 96. Photos. Exposed column-to-pile cap connection at pier P11 of the east bridge.

Source: FHWA.

A. Size of the opening.

Source: FHWA.

B. Damaged concrete.

Figure 97. Photos. Gap opening between the bottom of both columns and the top of the pile cap at pier P11 of the east bridge.

Source: FHWA.

Figure 98. Photo. View into the gap at the column-pile cap connection at pier P11 of the east bridge.

Apart from the damage to the column-to-pile cap connection at pier P11, significant damage also occurred at the bearing connections on the other piers. The superstructure appeared to have "jumped" longitudinally in both directions. There were indentations on both sides of the stiffener. As shown in figure 99, the large longitudinal movement of the bridge deck damaged the bolted connections of the steel bearings to the bottom flanges of the girders. Another consequence of this movement was that the web stiffeners were no longer aligned with the bearings, causing damage to the girder webs and flanges in the vicinity of the bearings. This type of damage was observed in both interior and exterior girders (figure 99 and figure 100). In addition, some bearings were also torn apart (figure 101). However, it appears that the failure of the bearings and/or their connections acted as a fuse, protecting the columns below from damage. As noted in the preceding paragraph, in the only case (pier 11) where the bearings and/or their connections did not fail, the pier below rotated and the pier-to-pile cap connection failed.

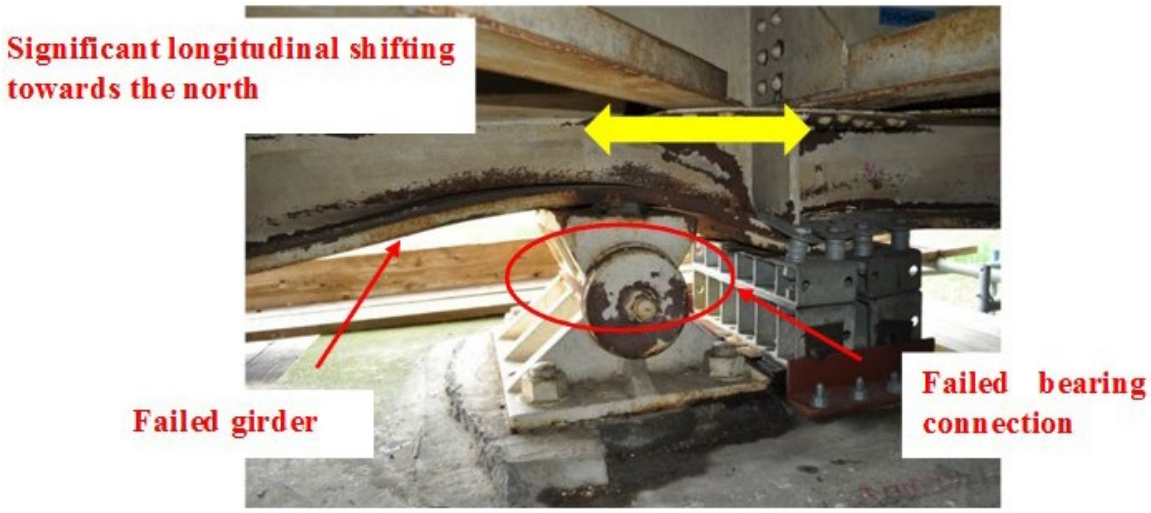

Source: FHWA.

Figure 99. Photo. Failed bearing connection under the west girder at pier P10 of the east bridge.

Source: FHWA.

Figure 100. Photo. Failed bearing connections under interior girders at pier P10 of the east bridge.

Source: FHWA.

Figure 101. Photo. Failed bearing connection under the east exterior girder at pier P10 of the east bridge.

Akitsu River Bridge

The Akitsu River bridge was constructed in 1976 and retrofitted between 2005 and 2007. The retrofit consisted of column jacketing, strengthening and widening pier cap beams, and adding additional seat width at the abutments and unseating prevention devices.

The bridge is on the Kyushu Expressway on the western side of Mashiki Town. It is oriented NS, with abutment A1 north and A2 south. The bridge has a steel plate girder superstructure that is 397 ft (121 m) in length with four spans (figure 102). The team only visited the northern abutment A1 (figure 103, figure 104, and figure 105). Abutment A1 is supported on steel pipe piles 31.5 inches (80 cm) in diameter. There are five rows of piles. The two rows at the back of the abutment are plumb. The three rows in the front of the abutment are slightly battered. Pile batter information is not available. Pile lengths are 69–130 ft (21–39.5 m).

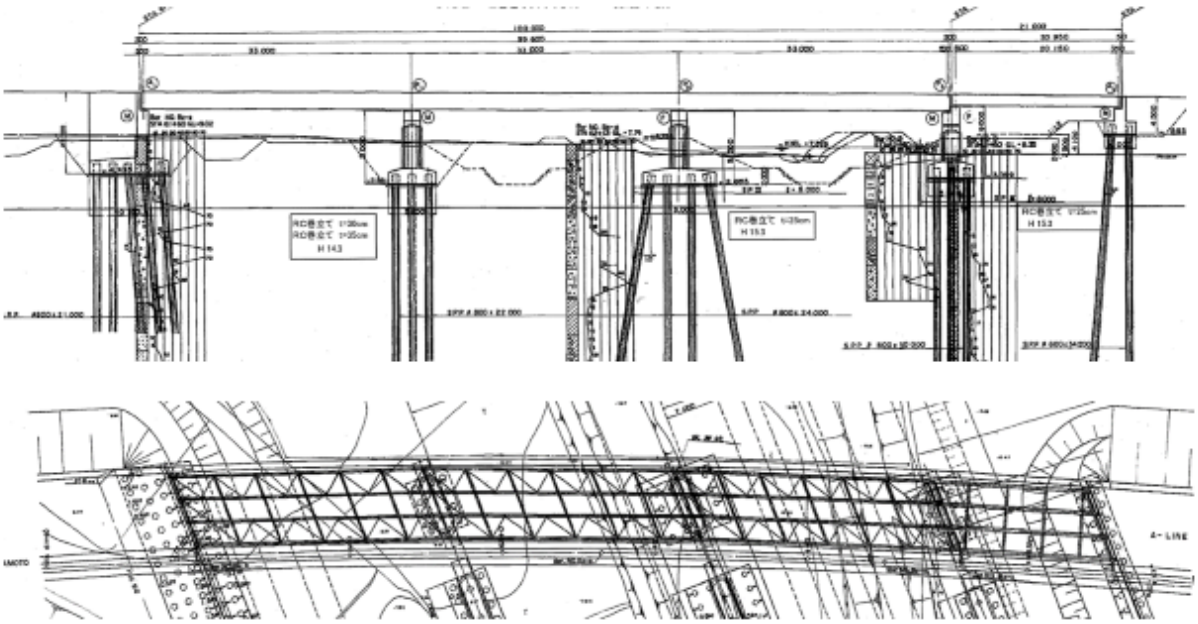

Figure 102. Drawing. Elevation and plan of Akitsu River bridge.[20]

[20]Ibid.

Source: FHWA.

Figure 103. Photo. General view of abutment A1.

Source: FHWA.

Figure 104. Photo. Side view of abutment A1.

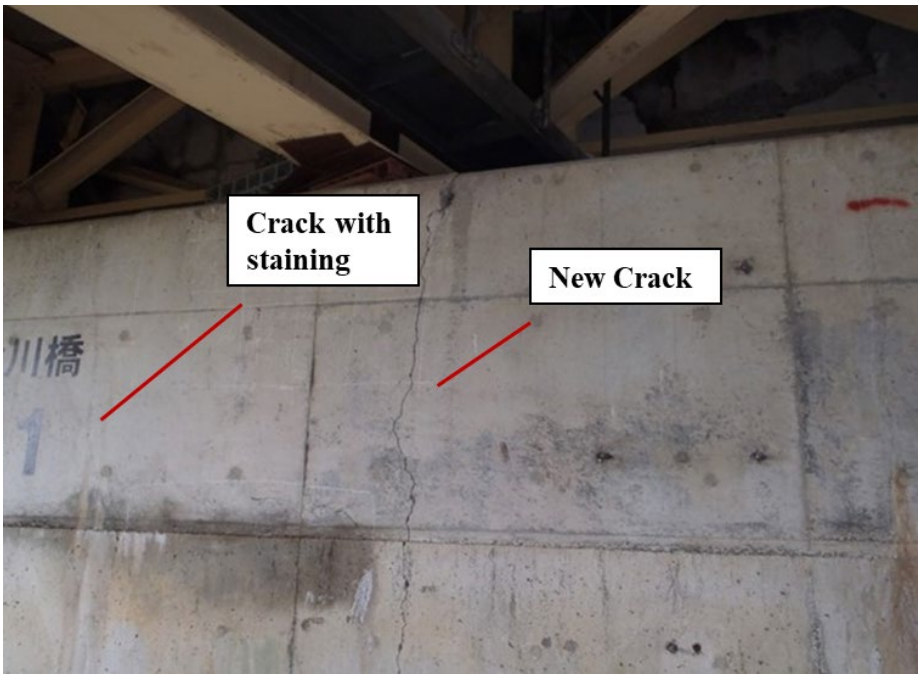

Source: FHWA.

Figure 105. Photo. Vertical cracks in the seat of abutment A1.

There were obvious signs of liquefaction and lateral spread at abutment A1 approach. There is a wall-lined canal in front of the abutment. The canal passes under the structure then turns north and parallels the east side of the approach. The canal wall closest to the abutment and approach was severely damaged. Lateral spreading moved the northern canal wall away from the abutment.

Abutment A1 has some vertical shear cracks that are shown in figure 105. One crack looks fresh, but adjacent to it is a similar crack with staining that has obviously been there a long time.

The entire superstructure was reported to have been displaced to the north. Coincident with superstructure displacement northward, abutment A1 may have displaced southward. As a result, the back wall of the abutment was damaged, the bearings suffered damage, and the girder stiffening plates were no longer aligned over the bearings, which resulted in damage to the bottom flange and web of the girder (figure 106).

Source: FHWA.

Figure 106. Photo. Damaged expansion bearing and girder at abutment A1.

The approach fill was excavated to gain access to the abutment wall for demolition and reconstruction. Figure 107 shows the back of the abutment with the end wall removed. In the left of the figure, the curtain wall is shown still standing with shoring supporting the adjacent roadway.

Source: FHWA.

Figure 107. Photo. Bridge approach replacement.

Higashibaru Bridge

The Higashibaru bridge was constructed in 1971 and is located on the Kyushu Expressway (figure 108). It has three equal spans, as shown in figure 109 and figure 110. It was designed according to the S39 *Design Specifications of Reinforced Concrete Highway Bridges* (JRA 1964). It is a reinforced concrete hollow slab bridge with pin-pin columns, as well as external shear keys at the abutments.

Original Map: © 2022 Google®. Modified by FHWA (see Acknowledgments section).

Figure 108. Map. Location of Higashibaru bridge.

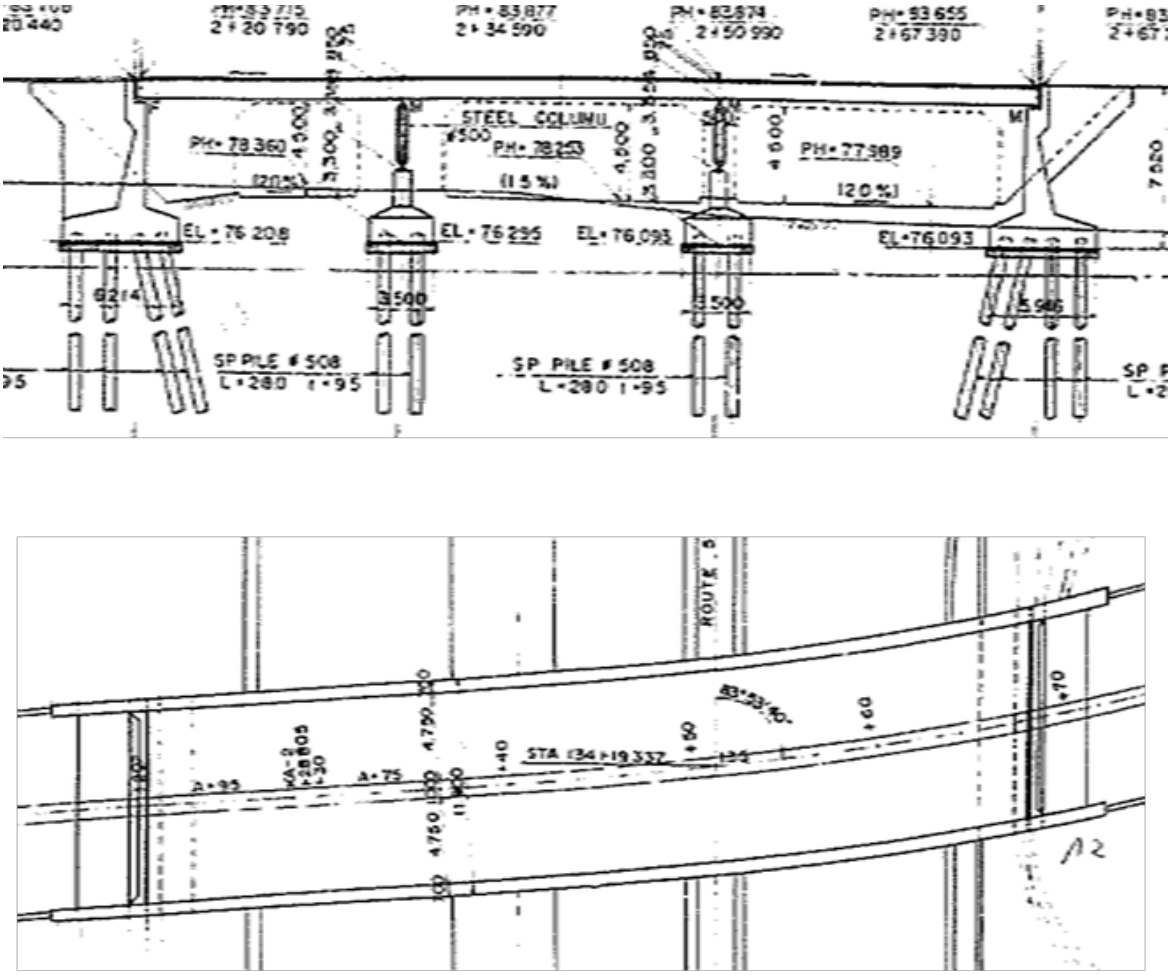

Figure 109. Drawing. Elevation and plan of Higashibaru bridge.[21]

[21]Ibid.

A. Pier before the earthquake.

B. Abutment before the earthquake.

Figure 110. Photos. Higashibaru bridge before the earthquake.

The team noted that several bridges crossing the Kyushu Expressway were of this type and no doubt were designed and constructed at about the same time (figure 111).

Source: FHWA.

A. Close-up of similar columns of a nearby bridge.

Source: FHWA.

B. Similar columns of a nearby bridge.

Figure 111. Photos. Another bridge with pin-pin columns near Higashibaru bridge.

Earthquake damage to the bridge consisted of permanent lateral deformations and damage to abutment A2 (figure 112, figure 113, and figure 114). Damage to the shear keys led to permanent lateral deformation of the bridge. There was no damage to abutment A1.

A. Inclined columns after the earthquake.

B. Inclined columns after the earthquake.

Figure 112. Photos. Inclination of pinned columns after the earthquake. [22]

[22]Ibid.

A. Close-up.

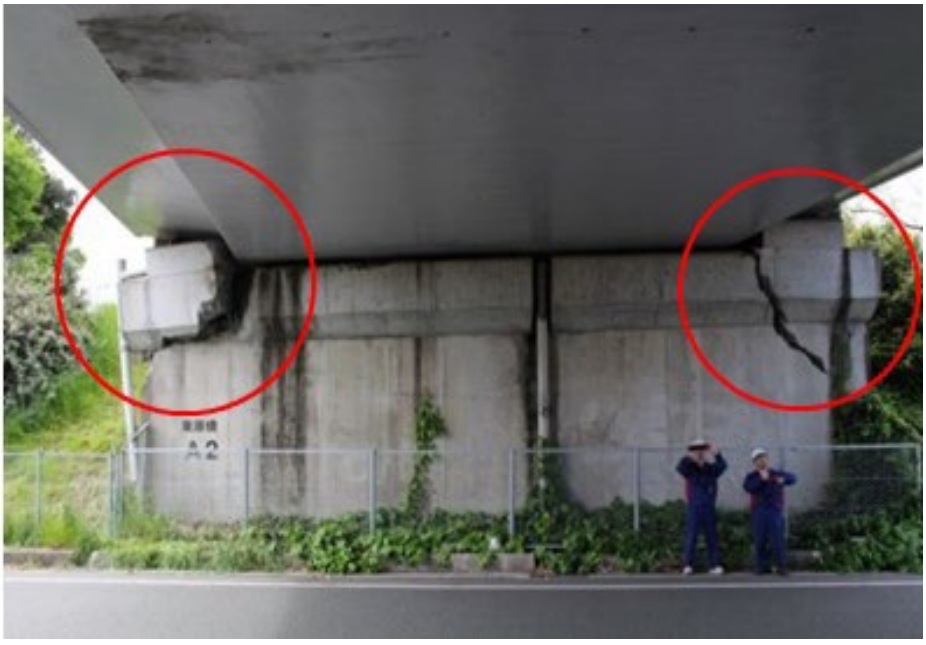

B. Overview.

Figure 113. Photos. Shear key damage at abutment A2.[23]

[23]Ibid.

A. Close-up.

B. Overview.

Figure 114. Photos. Side view shear key damage at abutment A2.[24]

[24]Ibid.

At the time the team visited the bridge, repairs had already occurred: the columns had been completely encapsulated in concrete (figure 115), and the abutment had also been repaired (figure 116). In effect, the bridge had been converted from a system with pin-pin columns to a pier-wall system with shear keys to constrain lateral movement.

Source: FHWA.

Figure 115. Photo. Repaired piers.

Source: FHWA.

A. Overview.

Source: FHWA.

B. Close-up.

Figure 116. Photos. Repaired abutment A2.

OTHER BRIDGES

Aso Oh-hashi Bridge

The Aso Oh-hashi bridge was a steel deck-truss bridge built in 1971 on Route 325 (figure 117). It consisted of five spans, including one arch span of 406.82 ft (124 m), and had a total length of 675.85 ft (206.0 m). Figure 118 and figure 119 are a rendering and a photograph of the bridge before the earthquake, respectively.

Figure 117. Map. Location of Aso Oh-hashi bridge.[25]

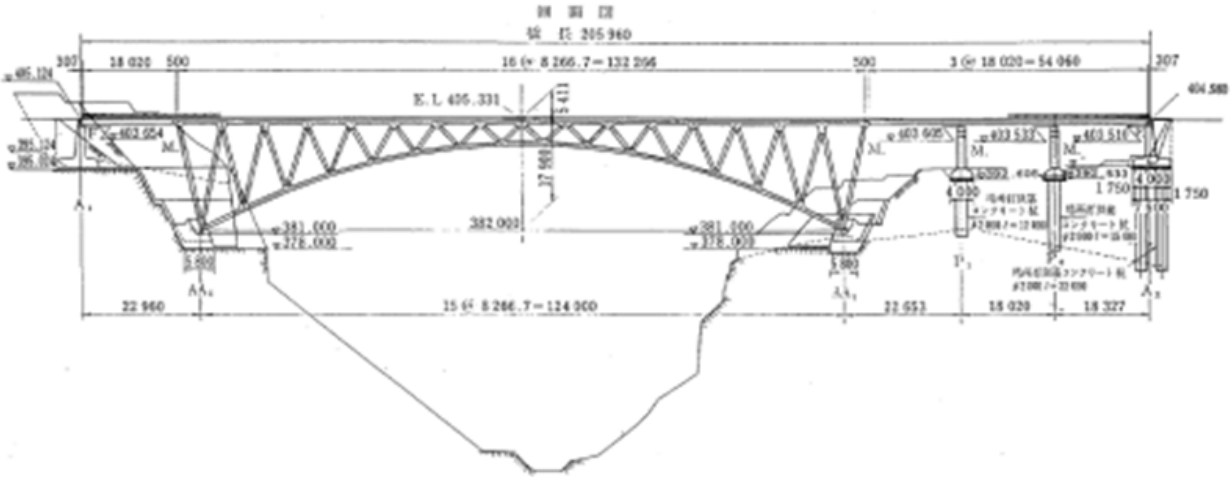

Figure 118. Drawing. Elevation of Aso Oh-hashi bridge.[26]

[25]Ibid.
[26]Ibid.

Figure 119. Photo. Side view before the earthquake. [27]

During the earthquake, a massive landslide occurred immediately upstream and above the west abutment. The arch springing just below this abutment was totally undermined, and it collapsed into the river gorge below, taking with it the remainder of the bridge. At the time of the reconnaissance, the east approach remained, and the views from this abutment are shown in figure 120 through figure 124.

[27]Ibid.

Source: FHWA.

Figure 120. Photo. Remainder of the approach slab at the east abutment.

Figure 121. Photo. Remainder of the east abutment and unseated first span.[28]

[28]Ibid.

Figure 122. Photo. Unseated first span below the east abutment.[29]

Figure 123. Photo. Seat and back wall of the east abutment and remainder of the expansion joint.[30]

[29]Ibid.
[30]Ibid.

Figure 124. Photo. Landslide upstream of the west abutment across the gorge causing bridge collapse.[31]

[31]Ibid.

CHAPTER 5. LESSONS LEARNED AND RECOMMENDATIONS

BACKGROUND

Roughly 180 bridges were damaged by the Kumamoto earthquakes, and a number of them were either recently constructed (15–20 yr old) or recently retrofitted.

Many of the new bridges that were damaged were located on a highway that had been realigned to improve access to a resort area. They were thus designed to the same specification and constructed about the same time (JRA 1996). Many of these bridges shared the same details, such as steel superstructures, elastomeric bearings, and reinforced concrete piers. This realigned road ran through steep, hilly country and was almost parallel to the Futagawa fault. Although no span collapsed on this road, damage sustained was significant, including bearing and shear key failures, steel superstructure distortion and local buckling, and foundation movement. The most likely cause was ground movement due to nearby slope failures and intense shaking in the near field of the causative fault.

Many of the retrofitted bridges that were damaged had only been partially retrofitted. For example, the piers of a multispan viaduct had been retrofitted with concrete jackets, but the steel pin bearings above the piers had not been strengthened or replaced. Many of these bearings failed. In another case, longitudinal dampers and transverse shear keys had been used to retrofit an arch bridge, but the abutment wall to which they were attached had not been adequately strengthened for shear, leading to a total loss of anchorage for the dampers. In this case, the weak link of the bridge system shifted from one component to another.

As far as can be determined, only 2 of the 180 damaged bridges had collapsed spans due to ground shaking. One collapse was due to a massive landslide immediately upstream of the bridge, leading to extreme debris loading on its foundation for which it had not been designed, leading to its total collapse. The other was a bridge with pin-pin columns, which suffered uncontrolled lateral displacements when the transverse stoppers at the abutments failed.

Bridge damage can be summarized as follows:

- Damage to bridges occurred due to intense shaking and/or extensive ground deformation associated with landslides.
- Observed damage patterns include:
    - Damage to bearings and bearing connections due to significant longitudinal and/or lateral displacement of either superstructure, substructure, or both.
    - Damage to bearings and bearing connections due to uplift and shear in curved steel girder bridges and a cable-stayed bridge.
    - Damage to shear keys and longitudinal restrainers.

- Buckling of steel girders (stiffeners, flanges), most likely due to uplift followed by horizontal impact of the girders on the abutment seats, and longitudinal impact of the girders on the abutment back walls.

- Significant lateral displacement of expansion joints and back walls of abutments due to ground deformation or impact of the girders on the abutments.

- Cracks at the base of reinforced concrete columns, but no spalling.

- Rotation of a jacketed pier and failure of the pier-to-pile cap connection.

- Total collapse occurred in only two cases and under extraordinary circumstances.

- Minimal column damage was observed due, in many cases, to one or more connection failures between the super- and substructures. These failures acted as fuses and protected the substructures from high inertial loads generated in the superstructure.

- Bridge performance overall was excellent, given the intense nature of the ground motions and unstable soil conditions at many bridge sites.

LESSONS LEARNED AND RECOMMENDATIONS

Seven lessons learned and associated recommendations are listed as follows:

1. Extensive landslides occurred throughout the Kumamoto Prefecture with detrimental effects on highway bridges. This widespread damage indicates the need for:
   a) Better understanding of landslides/slope failures.
   b) Probabilistic assessment of slope instability.
   c) Development of mitigation measures to stabilize vulnerable slopes.
   d) Investigation of landslide effects on structures and measures to minimize these effects, such as “flow-through” abutments.

2. Bearings and their connections should be designed for uplift, or combined uplift and lateral displacement, for certain types of bridges,.

3. Longitudinal restrainers and energy dissipation devices should be designed and installed to accommodate simultaneous imposition of large, relative displacements in both the longitudinal and transverse directions.

4. Partial retrofitting of a bridge is better than not retrofitting at all, but it should be followed by a full retrofit as soon as possible. All components in the load path should be strengthened accordingly (e.g., girders, cross frames, bearings, columns, footings, and piles), including connections (e.g., bearings-to-pier cap and pier-to-pile cap).

5. Inadvertent fusing of a bridge superstructure can protect a bridge substructure. This phenomenon has been observed in other earthquakes (such as the Maule 2010 earthquake in Chile) and confirms the validity of one of the Seismic Design Strategies in the *AASHTO*

Guide Specifications for LRFD Seismic Bridge Design, in which deliberate fusing is acceptable. Such a strategy deserves further exploration (AASHTO 2012).

6. Bridges with pin-pin columns can suffer from large, transverse displacements and potential instability if the shear keys at the abutments fail. Such bridges should be avoided unless a restoring mechanism can be devised, such as a posttensioned column.

7. Cable-stayed bridges with uneven spans and horizontal curvature have a complex dynamic behavior. They can become unbalanced if uplift occurs during shaking and cable tension is lost. This unbalance results in overstressing of certain cables and damage to different components of the bridge.

ACKNOWLEDGMENTS

The authors gratefully acknowledge the assistance of the following organizations and personnel with the successful completion of this reconnaissance exercise:

- NILIM and PWRI for technical and logistical support under the U.S.-Japan Cooperative Programs of FHWA, MLIT, and the U.S./Japan Natural Resources Panel on Wind and Seismic Effects.

- Drs. Junichi Hoshikuma, Masahiro Shirato, and Shigeki Unjoh (NILIM, PWRI) for generous assistance in the field and free exchange of expertise.

- Earthquake Engineering Research Institute and Department of Civil and Environmental Engineering, University of Nevada, Reno, NV, for additional financial support.

The map in figure 13 was modified by NILIM to show the Futagawa fault orientation and bridge sites.

The map in figure 14 was modified by NILIM to show to show abutment labels and orientation. The original map is the copyright property of Google® Earth™ and can be accessed from https://www.google.com/maps (Google 2016).

The map in figure 108 was modified by NILIM to show the location of the bridge.

Any opinions, findings, conclusions, or recommendations expressed in this report are those of the authors and do not necessarily reflect the views of the sponsors.

REFERENCES

AASHTO. 2012. *AASHTO Guide Specifications for LRFD Seismic Bridge Design, 2nd ed*. Washington, DC: American Association of State Highway and Transportation Officials.

Google®. 2016. "Google Maps" (web page). https://www.google.com/maps/, last accessed March 21, 2022.

Iwata, T., and K. Asano. 2016. "Near-Fault Strong Ground Motions During the 2016 Kumamoto, Japan, Earthquake." *Proc. American Geophysical Union* Fall: S53B-2867.

Japan Meteorological Agency. n.d. "Tables explaining the JMA Seismic Intensity Scale" (web page). http://www.jma.go.jp/jma/en/Activities/inttable.html, last accessed March 21, 2022.

Japan Meteorological Agency. 2016. "The 2016 Kumamoto Earthquake Summary" (web page). http://www.jma.go.jp/jma/en/2016_Kumamoto_Earthquake/2016_Kumamoto_Earthquake.html, last accessed March 21, 2022

JRA, 1964. *Design Specifications of Reinforced Concrete Highway Bridges.* Tokyo, Japan: Japan Road Association.

JRA. 1994. *Design Specifications of Highway Bridges.* Tokyo, Japan: Japan Road Association.

JRA. 1996. *Design Specifications of Highway Bridges.* Tokyo, Japan: Japan Road Association.

JRA. 2002. *Design Specifications of Highway Bridges.* Tokyo, Japan: Japan Road Association.

JRA. 2012. *Design Specifications of Highway Bridges*. Tokyo, Japan: Japan Road Association.

Kawashima, K. 1995. *Impact of Hanshin/Awaji Earthquake on Seismic Design and Seismic Strengthening of Highway Bridges*. Report No. TIT/EERG 95-2. Tokyo, Japan: Tokyo Institute of Technology.

Kawashima, K., M. Nakano, K. Nishikawa, J. Fukut, K. Tamura, and S. Unjoh. 1996a. "The 1996 Design Specifications of Highway Bridges." Presented at the *29th Joint Meeting of the Panel on Wind and Seismic Effects, May 13–16, 1997*. Tsukuba, Japan: Public Works Research Institute.

Kawashima, K., K. Nishikawa, M. Nakano, S. Unjoh, Y. Kimura, and J. I. Hoshikuma. 1996b. "Guide Specifications for Reconstruction and Repair of Highway Bridges Which Suffered Damage Due to the Hyogo-Ken Nanbu Earthquake." Presented at the *28th Joint Meeting of the U.S.-Japan Cooperative Program in Natural Resources Panel on Wind and Seismic Effects*. Gaithersburg, MD: NIST, p. 159–174.

Kawashima, K., and S. Unjoh. 2004. "Seismic Design of Highway Bridges." *Journal of Japan Association for Earthquake Engineering* 4, no. 3: 174–183.

Kuwabara, T., T. Tamakoshi, J. Murakoshi, Y. Kimura, T. Nanazawa, and J. Hoshikuma. 2013. *Outline of Japanese Design Specifications for Highway Bridges in 2012*. Gaithersburg, MD: National Earthquake Hazards Reduction Program, National Institute of Standards and Technology. www.nehrp.gov/pdf/UJNR_2013_Kuwabara_Manuscript.pdf, last accessed March 21, 2022.

Ministry of Construction. 1995. *Report on the Damage of Highway Bridges by the Hyogo-ken Nanbu Earthquake*. Tokyo, Japan: Committee for Investigation on the Damage of Highway Bridges Caused by the Hyogo-ken Nanbu Earthquake, Ministry of Construction.

NIED. n.d. "Strong-motion Seismograph Networks (K-NET, KiK-net)" (web page). http://www.kyoshin.bosai.go.jp, last accessed March 21, 2022.

NILIM. 2017. *Report on Damage to Infrastructures by the 2016 Kumamoto Earthquake.* Technical Notes NILIM 967 and PWRI 4359. Tsukuba, Japan: NILIM.

Okumura, K. 2016. *Earthquake Geology of the April 14 and 16, 2016, Kumamoto Earthquakes*. Hiroshima, Japan: Hiroshima University. http://home.hiroshima-u.ac.jp/kojiok/kumamoto2016KOreport2.pdf, last accessed May 4, 2022.

Rhea, S., A. C. Tarr, G. Hayes, A. Villaseñor, and H. M. Benz. 2010. *Seismicity of the Earth 1900–2007, Japan and Vicinity*. Open-File Report 2010–1083-D. Reston, VA: U.S. Geological Survey.

Shimokawa, K., Kinugasa, Y., and Tanaka, T. 1999. "Paleoseismology and Activity Study of the Hinagu Fault System, Southwest Japan," in *Proceedings of the Paleoseismology Workshop, March 15, 1999, Tsukuba, Japan*. USGS Open-File Report No. 99-400, GSJ Interim Report No. EQ/99/2.

Taira, A. 2001. "Tectonic Evolution of the Japanese Island Arc System." *Annual Review Earth Planetary Science* 29: 109–134.

Unjoh, S., T. Terayama, and JRA. 2002. "2002 Design Specifications for Highway Bridges," in *Proc. 34th Joint Meeting US-Japan Panel on Wind and Seismic Effects*. Special Publication 987. Gaithersburg, MD: National Institute of Standards and Technology, p. 231–240.

USGS. n.d. "M 7.0–6 km ESE of Kumamoto, Japan" (web page). http://earthquake.usgs.gov/earthquakes/eventpage/us20005iis#region-info, last accessed March 21, 2022.

Wei, D., and T. Seno. 1998. "Determination of the Amurian Plate Motion," in *Mantle Dynamics and Plate Interactions in East Asia, vol. 27, Geodynamics Series,* ed. M. F. J. Flower, S.-L. Chung, C.-H. Lo, and T.-Y. Lee. Washington, DC: American Geophysical Union, p. 337–346.

Recommended citation: Federal Highway Administration,
Performance of Transportation Infrastructure During Kumamoto Earthquakes of April 14 and 16, 2016—A Reconnaissance Report
(Washington, DC: 2023) https://doi.org/10.21949/1521940

HRDI-30/03-23(WEB)E